EXPERIMENTAL FLUCTUATIONS IN THE IONIZATION OF COSMIC RAY PARTICLES IN A THIN FOIL

Thesis by

Melvin L. Merritt

In Partial Fulfillment of the Requirements

For the Degree of

Doctor of Philosophy

California Institute of Technology

Pasadena, California

1950

ACKNOWLEDGEMENT

Credit and thanks are due the Office of Naval Research who have supported this work under Contract ONR Physics 13. I am also indebted to the Institute, which has contributed to my financial support during these past four years by a tuition fellowship and graduate assistantship.

Especial thanks are due to Mr. Robert C. Jopson with whom this work has been done and who has been a fine fellow worker. To Dr. E.W. Cowan who built the electronic circuits and to Dr. R.V. Adams who directed our work in the beginning, thanks. For ideas and criticism at the right times, for his direction of my efforts, I say thank you to Dr. Carl D. Anderson.

ABSTRACT

On an exploratory basis, a cloud chamber has been controlled in its operation by a proportional counter mounted within it. As a selection device for events of high ionization this has been satisfactory, and information is given on the types of events actually observed.

The ionization produced in the counter by single particles is shown to be subject to wide fluctuations. These are discussed with reference to existing theories on energy losses, but it is shown that calculations based on these theories are not wholly applicable to this case, as the foil represented by the gas is too thin. To these fluctuations is attributed the large proportion of single particles seen in resultant pictures.

TABLE OF CONTENTS

I. INTRODUCTION

1.1 Historical

Instruments of physics are rare which will give information on single events; the majority rely on a statistical aggregate of many. Those that do exist deserve loving care in their development and painstaking care to use them to their fullest. Such an instrument is the Wilson cloud chamber and experiments directed towards improving its operation and versatility have been carried on for a long time.

The cloud chamber grew out of early experiments of C.T.R. Wilson and others (1) who were investigating the process of drop formation in clouds. Progress towards its present use started when it was noticed that drops form on the ions formed by nearby x-ray activity; by 1911 Wilson was able to photograph the tracks of α-particles and fast electrons, and by 1927 Skobelzyn (2) observed tracks which later were shown to be due to cosmic ray particles. Since this time the cloud chamber has been used by many workers in the field of cosmic ray physics.

Simultaneously another tool useful in this field had been developed, the Geiger Müller counter. It also responds to single events in nature, but on the more crude yes-or-no basis. Its particular field of usefulness has been in questions in which very much statistical information is needed.

A particularly great advance in method was made in 1932 by Blackett and Occhialini (3) in combining these two tools by arranging counter-controlled expansion of a cloud chamber. Previously the chambers had been expanded at random, and only a tenth or a twentieth of the pictures showed any cosmic radiation, whereas after that it was possible to have virtually every picture meaningful. Today very few cloud chamber experiments are carried out without some measure of control over their operation by one or more Geiger counters.

1.2 Present purposes

The particular apparatus used in the work here described has experienced much of this development of methodology. It was built in 1930 by Dr. Carl D. Anderson (4); and, operated randomly, it gave pictures with which he proved the existence of the positron. Since then it has been used in other researches over the course of the years.

After the last war, this chamber and its magnet were mounted in a B-29 airplane and flown at high altitude. One summer's work in 1947 resulted in publishable data (5).

In the summer of 1948, attempts were made to determine the mass and the decay products of the meson, but the control equipment unfortunately did not discriminate adequately against showers. A few slow mesons were seen and no decays. In addition, the amount of time we were able to stay at altitude was extremely small. The apparatus was therefore removed from the airplane and returned to Pasadena.

We then decided to place a proportional counter within the cloud chamber. The fact that this instrument responds proportionally to the ionization produced within it might give added useful information, and it should prejudice the equipment in favor of low energy events of the type in which we were interested. In addition, so far as we knew proportional counters had never been used to control the expansion of cloud chambers and it was time to try. Recent years had brought developments of electronic techniques that should enable one to detect the passage of a single minimum ionizing particle.

To this end Dr. E.W. Cowan built the necessary electronic equipment and the author built the necessary counter. With this control the equipment has been operated for more than a year. It has not operated quite as had been expected. Readings on the ionization of individual particles were not useful, as they were subject to too great fluctuations. On the other hand, it is felt that the proportional counter has been and should continue to be a useful device for the control of cloud chambers, an extension to the versatility of their use. There have been many interesting pictures; Mr. R.C. Jopson is presenting an analysis of some of these in his thesis. The question of the nature and magnitude of the fluctuations and how they affect operation is the subject of this thesis.

II. APPARATUS

2.1 General comments

The apparatus used is in its basic elements that made by Dr. Anderson and used extensively by him in Pasadena, in Panama, and on Pike's Peak. The chamber and magnet are his original; various auxiliary elements have been added during succeeding years, and the electronic control elements in 1949. It has been described repeatedly (4,6), so that the description here will be sketchy except for the very recent additions.

2.2 Basic components

A chamber 7" in diameter and 2" deep is mounted vertically in the field of a large water-cooled electromagnet. Illumination is provided by the discharge of condensers through GE FT-127 flash tubes, the light passing between the pole faces of the magnet. Photography is through a rectangular hole cut axially in one pole, with mirrors along the sides of the hole to provide stereoscopic views.

The chamber is filled with a mixture of argon and helium at a pressure of three atmospheres and saturated with ethanol vapor. When a solenoidally operated mechanical trip is fired, the differential pressure between this and a vacuum chamber behind the chamber piston causes the latter to move. This motion takes place within 4 to 6 milliseconds depending on the amount of damping at the end of its motion. After expansion an automatic timing system takes over, the light is flashed, and then the chamber is recompressed and set in position for a new expansion. This period including recovery time is 38 seconds.

2.3 Safety devices

Especially developed for this series of experiments were a series of safety devices. When the chamber was operating in a B-29, it was necessary as well as practical to have an operator in immediate attendance at all times, for it was operated for relatively short, concentrated periods, and under variable conditions. When installed at the Institute, however, it was expected that the external conditions would be relatively constant over long periods of time, and it was hoped that continuous operation would be possible. Under such conditions continuous personal supervision was manifestly impracticable. A necessary item of equipment then was a series of safety devices of some sort.

The particular troubles anticipated that we wished to guard against were these: the flow of cooling water to the magnet might be impeded and the magnet burn up, the magnet voltage might vary overmuch and negate any curvature measurements, a hose might break or leak and flood the room, or the chamber might fail to reset and injure itself by repeated attempts to do so. As a matter of actual practice the only one of these troubles which has never occurred is that of a large variation in magnet voltage. In order to guard against these things, the series of circuits given in Fig. 1, a & b were designed and constructed.

The normal sequence of operation with everything operating correctly is as follows:

1. Push switch S1. This turns on the 24 volt D.C. and the 100 volt 400 cycle generator.
2. Push switch S2. This is a necessary preliminary to S3, as the holding circuit of Relays K1 and K2 will not hold unless circuit D is closed. This operation is dependent on either the 24 v. D.C. or the 110 v. D.C. or both being on, and was added because it was desired that the whole equipment could be turned on even when the magnet voltage is not on and that safety circuits still be operative then.
3. Before proceeding it is necessary that the magnet cooling water be on.
4. Push switch S3. This activates all safety circuits. It is now possible to close the appropriate solenoid so that voltage might be applied to the magnet; before it was not so possible.

If while in operation one of the enumerated troubles should occur, the safety devices will turn the equipment off in the following manner:

1. If the water flow ceases, it will no longer fall into a leaky catch bucket, hence will no longer depress a micro-switch on which the bucket is supported and will open the circuit at A, open relays K1 and K2, open the magnet field relay circuit, hence interrupt the magnet current and the magnet will not burn up. The 110 v. D.C. having also been on, condenser C1 will discharge through relay K3, open it momentarily and turn off all other power

as well. When this happens the water will also be turned off at the tap by a solenoidally operated valve.

2. If the magnet gets too hot, by reason of partial stoppage of water or anything else, then one of two things will happen: either a thermally operated switch in the exit water line will open and cut all power off, or if this fails, a Wood's metal link in thermal contact with the magnet coils will melt and open the circuits.

3. If the 110 v. D.C. voltage to the magnet gets too great, relay K5 will open circuit D.

4. If the 110 v. D.C. voltage gets too small or goes off entirely, relay K4 will open circuit D.

5. If water gets on the floor, it will act on switches set in the most likely low spots about the equipment. These switches are essentially a spring-loaded switch, held closed by a small piece of Alka-Seltzer tablet. These are very water-sensitive.

6. If the chamber fails repeatedly to reset due to loss of air pressure or any other such mishap, the circuits of Fig. 3 take over. The essential element is a motor M1. Every time the chamber fires it starts to run forward. If the chamber resets satisfactorily it reverses, and returns to standby position; if not, it continues, giving the chamber time to make 4 to 8 attempts at resetting, then turns off the timers.

These circuits have worked satisfactorily whenever they have been needed.

2.4 Counters

The counter control over this series of experiments has been a combination of several Geiger counters and one proportional counter. The Geiger counters used are those familiarly called "Neher counters" in this laboratory and described previously (7).

The proportional counter was built for this experiment by myself. To improve our selection, we wanted to put the counter in the very middle of the chamber. This required that the counter be small as the chamber is small, and that it have a rectangular cross-section so that the absorbing thickness would be definite. It should present a low absorbing thickness so that identification of particle type and measurement of momentum should be definite, and be of low atomic number so that we should not have to worry about radiation energy losses but only about ionization energy loss.

All this suggested that the counter be built of aluminum. This was done; the details are best seen by reference to Fig.2. This final model has an internal active space 7/16" (1.1 cm.) thick, 1-1/16" (2.7 cm.) wide, and 3" (7.6 cm.) long. Its walls are each 0.065" thick giving an absorption thickness of 0.89 gm/cm^2. This thickness was about as thin as it could be made and still be strong enough so the flat walls would not distort appreciably when filled to a high internal pressure. The problem of soldering to the aluminum was solved by first plating it with copper using a cold Rochelle strike as recommended by the Aluminum Company of America. It then could be easily handled by the usual tin-lead solder (8).

Details of the mounting are given in Fig. 3. The essential problem here was to mount the tube on a cylinder of glass and to lead out a shielded electrical connection. This is the reason for the curved washers and the flexible coupling: several rings were broken before this was tried. It was also necessary that this be of a form that could be assembled in the narrow space between the poles with the chamber in place.

The counter was filled to an inside pressure of three atmospheres of 90% argon, 10% CO_2.

2.5 Electronic circuits

Electronic circuits were designed and built by Dr. E.W. Cowan. These circuits are reproduced schematically in Fig. 4 a to f. Figures 4 a and b are conventional power supplies. Fig. 4c shows the preamplifier. The design of this is the most delicate of all, for on its stability and reliability depend that of all that follows and of all the data obtained. There is heavy degenerative feed back and a special regulated filament supply to help assure these things. Its output is through a cathode follower to the main amplifier, Fig. 4d, which consists of two chains of three tubes, each with degenerative feedback. Fig. 4e shows the gate and coincidence circuits. These require that one or both Geiger tubes fire at the same time as the proportional counter, in this way defining a solid angle within which the particle must lie. The composite signal is then fed through a cathode follower to three circuits (Fig. 4f) one of which decides if the signal is high enough to fire the chamber and the other two of which measure the height of the pulses. Each of these is in essence a long time constant peak reading vacuum tube voltmeter, but one has a two-tube preliminary amplifier with a gain of 5, so that the two circuits and their associated indicator meters act as fine and coarse scale meters with a 5:1 scale ratio between the two.

2.6 Recording camera

To record the information on height of pulses given by the proportional counter, a Bell and Howell Eyemo 35 mm. movie camera with an f/2.8, 2" focal length lens was used, which camera was loaned from the facilities of the N.O.T.S. at Inyokern. Its operating solenoid was pulsed so that single frames were taken of each item of information.

III. OPERATING CHARACTERISTICS

3.1 Calibration

For pedagogical purposes ionization chambers, proportional counters, and Geiger tubes are often considered as like instruments used under different circumstances (9). One then discusses the behavior as one raises the externally applied voltage, and shows how it passes through these various types of operation and then ends in continuous breakdown. This is a useful description in that it stresses the similarities of operation as against the factors which cause the various modes of operation to be different, but it avoids the great differences in choice of filling, in external circuits used, etc. The proportional counter differs from the ionization chamber, for instance, in that the size of the voltage pulse has been amplified by internal ionizing collisions. For true proportionality this amplification is independent of the original number of ions formed. In this respect the Geiger counter differs from the proportional counter. For the former amplifies in such a manner that the output pulse size (not the amplification) is independent of the original number of ions formed. This is usually attributed to the emergence of factors other than collision that produce or inhibit the production of new ions.

The usual difficulty in using proportional counters to detect cosmic ray particles is that these ionize very little compared to alpha particles or the like, for which they are often used. This has been avoided as much as possible by using a high-gain amplifier, but even more by using a large gas pressure. This results of course in more ions being originally formed, so that the initial pulse, even not multiplied, is larger. To test the proportional regions of operation of the counter and its associated circuits the following method was used. It does not involve artificial sources; these were not used as they do not involve <u>single</u> high energy particles. The counter was set up on a bench in coincidence with two Geiger tubes and the sizes of the pulses obtained were recorded. This was done for both the wide and for the narrow dimensions of the counter and the results compared (a typical result in Fig. 5). The results were that the peaks lay in a ratio of about 2; i.e., in about the ratio of the two dimensions of the counter. As these peaks represent the most probable ionization loss, and as this should be proportional to the distance traversed, this was taken to indicate that we were indeed within the proportional region of the operation. The final choice of operating voltage was on the basis of avoiding noise as well as the above; we tried to strike a balance between gas and electronic amplification.

At the beginning it was thought desirable to know what the meter readings indicated. Thus did a value of 8 mean an ionization of 8 x minimum, or what? This was originally done by such graphs as Fig. 6. This particular one was made with a different metering circuit than is shown in Fig. 5, but the essential features are the same. This particular one would indicate that a meter reading of 2 corresponds to the most probable ionization for a fast cosmic ray particle. Such tests were repeated later to check on the constancy of performance.

3.2 Results of operation

Our control circuits provide that the chamber will expand only when particles appear from the vertical, ionizing as they go more than a certain predetermined minimum. We might speculate on what might mainly be expected to be found in the resultant pictures. If the bias were low, one would expect the same distribution of events as a Geiger tube in the same place as the proportional counter would give, except that if the bias were too low blank pictures would appear due to noise in the circuits. These pictures would be of single particles plus showers, etc., in their usual relative abundance. If on the other hand the bias were higher, the counting rate should go down, and the remaining pictures should be of those events characterized by high specific ionization. These might be low energy protons or mesons, showers, pairs, or stars. The relative number of single particles would be expected to go down sharply.

As a matter of practice the distribution of the various types of events does change, but not quite as expected. In Tables I, II, and III are given some data on this. The particular 14 rolls of pictures chosen for this comparison comprise a total of 6365 pictures taken during the period of July 11, to September 18, 1949. This interval was one relatively free of electrical and mechanical troubles, and one in which no changes were made in operating conditions that might af-

TABLE I

DISTRIBUTION OF TYPES OF EVENTS OBSERVED

Rolls 19-33

Gain	Singles	Doubles	Triples	Showers small	Showers large	Blanks	Uncertain	Other Types
1/4	58		1			21	7	
1/8	65	1				12	3	
1/16	406	2		2	1	13	26	3
1/32	224	6		3		4	22	2
1/64	3799	197	20	365	99	416	434	153

TABLE II

PERCENTAGE DISTRIBUTION OF TYPES OBSERVED

Gain	Singles	Doubles	Triples & Showers	Blanks	Uncertain	Other
1/4	66.7		1.1	24.1	12.1	0
1/8	80.4	1.2	0	14.8	3.7	0
1/16	89.6	.5	.7	2.9	5.7	.7
1/32	86.0	2.3	1.1	1.5	8.4	.8
1/64	69.3	3.6	8.8	7.6	7.9	2.8

TABLE III

DISTRIBUTION OF "OTHER" TYPES OF EVENTS AT 1/64 GAIN.

Mesons:	42 positive of which 16 show decay electrons.
	32 negative of which 3 show decay electrons.
Protons:	67 by themselves.
	6 in showers.
Stars:	6.

fect these tables. What is being compared here are the results for the same value of the bias setting but different values of the gain setting. This amounts to the same thing as mentioned above, for either thing varied will control what fires the chamber.

Pictures have been classified as to what appears to have fired the central proportional counter. Those labelled "blank" are those in which it cannot be definitely said that any visible track did so, though in some of these cases nearby fragments of tracks indicate that a shower may have been passing by. These blanks tended to decrease in relative abundance as the rigidity of selection increased. Those labelled "uncertain" are ones in which classification was doubtful or difficult; these stayed at about the same level. Multiple events are subdivided into doubles, which are mostly electron pairs or knock-ons, and showers, which were rather arbitrarily called small or large, the borderline being roughly a ten particle shower. Such events increased, as indeed they were expected to do.

It is of interest that there remains a large fraction of the pictures in which apparently one particle alone fired the chamber. The majority of these are cases in which the one particle visible is a high momentum particle; that is, it is very straight ($pc > 300$ Mev) and it appears to be a minimum ionizing particle. Visual estimation cannot determine any appreciable change in the appearance of tracks from minimum ionization up to about three times minimum, so that it might be supposed that some of these singles are these. This is considered later*; it is a valid comment, but the relative numbers of such are small. One might hypothesize that there are accompanying particles, of a shower perhaps, which are not seen. Such is improbable, however, for the entire area of the counter is within the illuminated area. One might hypothesize accompanying neutral particles. Photons, however, almost always accompany showers, and in any case would not produce an effect except by creating pairs or by Compton scatterings, both of which have been excluded in this classification. Neutrons could produce an effect if it were imagined that the results of their interaction were cast out in the long direction of the counter or straight backwards or frontwards. These mentioned possibilities are however secondary effects; the primary effect is that of fluctuations in the ionization of the individual particles. Of this more later.

The last column in Tables I and II, headed "other" types of events, includes events of the kind originally sought. These are subdivided in Table III. Out of 5483 pictures at 1/64 gain, covering an operating period of 1200 hours, there were 74 which contain mesons definitely identifiable by increased ionization, there were 73 showing protons near the end of their range, and there were six showing stars or possible stars. Of these 74 mesons, 19 were observed to decay in such a manner that their decay electrons were visible and identifiable, and it is probable that at least as many more decayed in other directions. These were the pay-off and the justification

---

* See the last paragraph of Appendix B.

for the labor and time. It is to be noted that this equipment has been used now for almost twenty years. In nineteen previous years, only two meson decays were observed (5, 10), and these two at an altitude, whereas now with a proportional counter controlling its expansion there have been some 19 in a space of only 7 weeks' operation. In the whole year, which has not been at all as continuous in operation as these particular 7 weeks were, there have been observed about 70.

3.3 Advantages and disadvantages

The advantage of proportional control of cloud chambers is pragmatic: it works; it does select low energy events. Speculation has run at times to what might have been seen if the chamber had had a larger active volume, but these are dreams and have no place here.

The disadvantages of this control system are in its difficulty of operation and are primarily due to the very small voltage pulses from the proportional counter. Because of this the amplifier circuit must be of very high gain. Its input impedance is high (in this case 800 megohms) so that it picks up noise easily. Its stability must be guarded, especially at the input. Then the tube itself and its mounting give some troubles. Actually the tube was easier to make work the first time than a Geiger counter using the same envelope, for its filling is less critical; indeed in the criterion of lifetime it is superior for there is no organic vapor to be used up. But troubles came from the absolute cleanliness necessary: the slightest bit of dust or water or grease film across any of the insulators or the glass seals produces spurious pulses which resemble the breakdown of Geiger tubes at high voltages. This was a source of trouble at the beginning and has been repeatedly since. To avoid this the glass seals at the ends of the counter were covered with Ceresin wax, and there are used a minimum number of very clean polystyrene washers to support the lead out to the pre-amplifier. It was also necessary scrupulously to avoid sharp corners and small internal spacings.

Nevertheless when these things are avoided there have been prolonged periods of quite satisfactory operation, witness the one cited above.

IV. FLUCTUATIONS

4.1 Background on theory

The problem of determining the distribution in energy loss of fast electrons was apparently first undertaken by Bohr in 1913 (11). On the basis of classical theory and the Rutherford-Bohr model of the atom he derived an expression for the cross-section $\sigma(E)$ for energy loss of electrons and α-particles. This turned out to be proportional to $1/E^2$ except for very small or very large values of E. He also got formulae for the mean energy loss including relativistic corrections and for the mean square fluctuation in energy loss in terms of this cross-section and the thickness of the material. From these he worked out correct formulae for mean range and for straggling in range of electrons and α-particles. For α-particles he showed that the energy loss distribution (except for very thin thicknesses, the present case) was essentially a Gaussian distribution. This result depended on the fact that the energy loss per collision of an α-particle with an electron was small. For electrons, which can transfer a major fraction of their energy, this is not so, so he modified his analysis by treating separately cases in which the energy transfer is small and in which it is large. For the small energy transfers he got again a distribution that was approximately Gaussian; the effect of large energy transfers was to increase the high energy tail of the distribution curve, to make it skew.

Bohr's treatment of straggling was taken up and extended by Williams in 1929 (12) and the following two years. Williams reconsidered in greater detail the question of high energy transfers, and showed that the contribution due to these could be expressed in a series, the nth term of which was the contribution of a particle suffering n such collisions. He then combined the two groups of energy losses by probability theory, treating them as independent random variables and obtained an explicit form for the probability $P(E,t)$ of an energy loss of E in a thickness of material t. He found $P(E,t)$ to be easily expressible in terms of a new universal function ϕ, such that

$$P(E,t) = \frac{1}{\xi}\,\phi\left(\frac{E-E_p}{\xi}\right)$$

where $\xi = At$ and $E_p = \xi\left(\ln\frac{\xi}{\epsilon} + j\right)$

(This notation is not his, but is due to Landau and to Symon.) The quantity j is a new universal constant he found to be 0.30, and A and ϵ are functions of the material traversed. E_p amounts to the most probable value of energy loss and ξ to a standard measure of fluctuations. Williams compared this result with experimental data on electron straggling. The theory gave the correct shape of the observed data but gave too small a magnitude of straggling (i.e., of the factor A) by a factor 2:3. This he attributed at the time to a failure of the classical theory to describe correctly low energy loss collisions.

In two later papers (13) Williams has compared experimental and theoretical results for the stopping of α- and β-particles. In the first of these he also compared the classical cross-section of Bohr with some new quantum mechanical calculations which had been made by Gaunt (14). The two agreed except for energies comparable to the atomic energy levels. The average energy loss was about the same in both theories, but whereas the Bohr theory had treated losses as continuous and finite for low energies, the quantum mechanical treatment found these losses to be concentrated in several resonance peaks and zero elsewhere. This probably accounts for some of the discrepancy between Williams' theory and experimental results mentioned above. Later, by a synthesis of Bohr's classical formula with a non-relativistic quantum mechanical treatment by Bethe (15), Williams arrived at a formula for the mean rate of energy loss which agreed with that obtained later by Møller (16) by a more rigorous treatment. This formula was also in satisfactory agreement with experimental data.

More recently Landau (17) has given a rigorous treatment of the problem of getting the energy loss distribution for high energy particles in fairly thin foils. He assumed the crossection for energy loss $\sigma(E)$ to be proportional to $1/E^2$ for E large compared with ionization potentials of the material traversed. For smaller values he took the energy loss as given by the relativistic Bethe formula and said that fluctuations due to these can be neglected. This assumption is fine except for particle velocities comparable to those of atomic electrons and <u>except when the expected fluctuations (ξ) are of the order of the ionization potentials.</u> Then if the dependence of the cross-section $\sigma(E)$ on the energy of the ionizing particle can be neglected (this is all right for fairly thin foils), $P(E,t)$ can be obtained rigorously using Laplace transformation methods. This Landau did and evaluated the differential and integral distributions of energy losses for this case.

Even later Symon took up the problem (18). Landau's assumption that the cross-section energy transfers varies as $1/E^2$ is only valid for energy losses ~~and~~ small compared to the maximum transferable energy E_m. As a result Landau's results were not applicable to large thicknesses of absorbers. Symon used more exact expressions for $\sigma(E)$ valid for large E and considered the variation of σ with the energy of the particle. He was able to present a series of curves which allow the determination of distribution of energy loss by ionization of mesons traversing thickness of matter up to 85% of their range. For greater thicknesses curves were given of the distribution in range of particles.

These statements have implied the type of problem in which these men were all interested. They were concerned with straggling in range, with the degree of inhomogeneity introduced by a thin foil into an originally homogeneous beam of particles, or in the probability distribution of the initial energy of a particle if its energy is known after having passed a known thickness of material. The problem of our interest does not agree except incidentally with any of these. Our present problem is the fluctuations in the energy left in the gas of a counter when cosmic-ray particles pass through and the effect this has on counter control of cloud chambers. Here there are essential differences in points of view. Primarily, the absorbing thickness represented by the counter gas is very small, near or past the lower limits of thicknesses for which these theories are valid or in which these men were interested. Then there is the unknown effect of having two much thicker absorbers, the counter walls, on either side of the gas and the possibility that ~~the~~ some energy loss processes (such as the production of δ-rays) will not be totally enclosed in the space of the counter.

4.2 Application of theory

Of the theories mentioned above, those due to Landau and Symon appear to be the most valid. In the region of very thin absorbers these two agree identically: Symon's results are generalized from Landau's towards application to thick absorbers. I propose to find what distribution in meter readings would be expected on the basis of this theory. It will turn out that this is an unjustified extrapolation beyond the limits of validity of the theory, justifiable only because no theory does describe this region satisfactorily.

The theory gives us a function $P(E,t)$ which is the differential probability that a particle with a given initial energy will lose an energy E in passing an absorbing thickness t. For our purposes, the thickness t is a constant, but the initial energy is not. Let us then express this function in terms of the variables E and p: we get a form $P(p,E)$. What we desire is $N(\varepsilon)\,d\varepsilon$, which is the probability of there being an energy loss between ε and $\varepsilon + d\varepsilon$. Now if we have $n(p)\,dp$ particles in the momentum range from p to $p+dp$, and the probability of one of these losing an energy between ε and $\varepsilon + d\varepsilon$ is $P(p,\varepsilon)\,d\varepsilon$, then the contribution to $N(\varepsilon)\,d\varepsilon$ of this group of particles is

$$P(p,\varepsilon)\,n(p)\,dp\,d\varepsilon$$

or the total contribution is

$$N(\varepsilon)\,d\varepsilon = \left[\int_0^\infty P(\varepsilon,p)\,n(p)\,dp\right] d\varepsilon$$

As I have written it $N(\varepsilon)$ is not normalized. It could be by dividing by the normalization factor

$$\int_0^\infty n(p)\,dp$$

but for these purposes all that is desired is the shape of $N(\varepsilon)$ not its absolute magnitude.

For these calculations it is assumed that all particles passing through the counter are mesons. This assumption specifically excludes high energy electrons which might have contributed to Fig. 9. For a preliminary meson spectrum we use Wilson's results as extrapolated by Rossi (19,20). This cannot be used directly, however, for the equipment was on the first floor of a three story building, and there is an average thickness of 320 gm/cm^2 of concrete above. This shifts the whole spectrum down towards lower momenta, the peak moving from 600 Mev/c to 300 Mev/c. This resultant, plotted in Fig. 7, is used for $n(p)$ *. The process of getting $N(\varepsilon)$ consisted first

---

* This process is given in more detail in Appendix A.

of transforming $P(p,E)$ from graphs and tables which give it for fixed p and variable E to a form in which we have it for fixed E and variable p, then numerically integrating*. As a matter of practice it was easiest to change the variable of integration to the logarithm and integrate the following:

$$N(E) = \int_{-\infty}^{\infty} p\, P(p,E)\, n(p)\, d\ln p$$

The result is given in Fig. 8, and as a matter of interest the energy loss distribution for 2400 Mev/c is also shown on the same graph to show how this process has widened the expected curve.

4.3 Experimental curve

In tables 4a and 4b are tabulated meter readings for some 7358 pictures. These particular ones were selected because they were taken under uniform operating conditions and because these pictures apparently contained just one minimum ionizing particle apiece and nothing else. Compared to tables 1, 2, and 3, this means that only ones there included in the "single" class are here included. Omitted then are all obvious multiple events, blanks, and pictures of doubtful interpretation. The ones left are those which are normally passed over as dull and uninteresting, but they are also the ones which account for most of the operation of a cloud chamber.

In assembling these tables all pictures in about 20 rolls of film (10,000 frames, roughly) were visually inspected and

---

* Details in Appendix B.

TABLE 4a

READINGS ON COARSE SCALE METER

gain	5-10	10-15	15-20	20-25	25-30	30-35	35-40	40-45	45-50	50
G1/64	3063	781	400	200	96	49	32	16	11	165
G1/32	499	139	61	31	15	14	6	8	8	27
G1/16	295	46	34	18	10	7	6	6	7	34
G1/8	508	509	226	97	67	39	24	9	11	82

TABLE 4b

READINGS ON FINE SCALE METER

gain	5-6	6-7	7-8	8-9	9-10
G1/64	897	716	534	411	304
G1/32	47	39	31	24	7
G1/16	87	63	67	47	31
G1/8	3	8	1	11	5

classified. Then for singles in each different gain setting the readings were enumerated according to the groups indicated by the column headings in these tables. As we have already seen there were two meters, each giving readings on the same particle. One would expect then that the 5-10 grouping of the coarse scale meter would agree with the sum of the numbers observed in the corresponding fine scale groups, but this is not so, for some of the fine scale data had to be thrown as its amplifier went bad.

From these data it is desired to obtain a curve indicating the relative frequency of different meter readings. It turned out to be impractical to normalize these on a time basis, so instead the curves were fitted together, which was quite practical due to large overlaps. The greatest weight of course was given to those particular data based on the greatest number of points. Of the fine scale data, only those at 1/64 gain were used, as the others were based on too small numbers.

This leaves one question, how to draw a smooth curve at the lower end. This is known to turn over from the preliminary calibration (see fig. 6) and from the consideration that there is only an extremely small probability of a particle passing through and not losing any energy. The data on the 5-10 and the 10-20 figures at 1/8 gain, namely 508 and 509 frames respectively, are ambiguous on this score. According to these figures the curve could still be rising though not so sharply as it is to the right. The fine scale data that might settle this point definitely were, unfortunately, lost when that particular amplifier chose to go bad; the little that is left has no particular significance. But it is known that the curve must turn over; the preliminary calibration indicated that this was somewhere in the range 8 to 12, and the curve from the calculations of section 4.2 fits best in this region, so let us take the figure 10 as the maximum point of the curve.

The results of this curve fitting are all summarized in figure 9. The interesting thing is the very high tail to the curve. It is tied in with the large number of pictures taken with just one particle showing, and is in fact a restatement of the same problem reduced to numbers.

4.4 Discussion of differences between experiment and prediction.

In the two preceding sections there have been obtained an experimental and a theoretically predicted curve for energy losses. They are shown together in figure 10.

Now these two curves are really not derived for the same circumstances. The experimental curve is one which indicates variations in the amount of ionization actually found in the gas of the counter. The predicted curve is one which indicates how much energy the primary particle would be expected to lose there, which is not the same thing at all. Consider the mechanism of large energy losses*. A

* By a large energy loss or transfer is meant one in which the secondary electron receives enough energy to produce subsequent ions. A low energy loss is the case in which no subsequent ions are formed.

primary particle loses energy by transferring it to an electron of the gas and this electron dissipates its energy by ionization along its path. What the theory talks about is the energy lost by the primary particle by high and by low energy transfers. What the counter concerns itself about is the final ionization actually to be found in the gas. The second might be different from the first either if some secondary particle formed within the gas should pass out of the gas without having dissipated all its energy or if some secondary particles formed in the counter wall should pass into the gas. The first such effect would decrease a reading; the second would increase it.

The region of comparison includes the region from zero to forty times the most probable ionization. From the theoretical curve this most probable loss is about 6000 electron volts. In round numbers then the concern is in energy losses up to about a quarter of a million electron volts (.25 Mev). Let us consider what would happen to a particle of this energy due to the presence of a magnetic field and due to its limited range. The magnetic field was 6350 gauss; this would cause such an electron to move in a circle of radius 0.3 cm. The mean range for such a particle is 0.65 gm/cm^2 which would correspond to 13 cm range in the counter gas or to 0.023 cm range in the aluminum walls. These figures indicate that electrons of this energy formed in the last 0.023 cm of the wall might pass into the gas. Now the probability of such an electron being formed is mass dependent, and the layer of wall that is feeding electrons into the gas is roughly 12 times as thick in gm/cm^2 as the gas, suggesting that more electrons might be entering the gas than are formed in it. The situation is confused somewhat, however, by the fact that electrons entering the gas from the wall will be curved around by the magnetic field and may reenter the wall. As to electrons formed in the gas, those formed in a central region have no possibility of escaping; they are constrained to moved in circles entirely within the gas of the counter. The conclusion is that the edge effects will increase the tail of the expected curve by an unknown amount.

It is seen that the experimental and the theoretical curves differ considerably. Why? It has already been hinted that the theory was not applicable. Symon's criterion for the lower limit of applicability of his theory was that

$$\xi > 5I$$

where

$$\xi = \frac{Ne^4}{mv^2}\frac{Z}{A}\rho t$$

and I is the average ionization potential as used in the usual formula for mean energy loss. Now I for argon is about 190 electron volts and ξ turns out to be in the order of 390 electron volts. We see then that this case is somewhat beyond the limit of applicability of that theory. Physically this criterion is tied in with the requirement that the material should be thick enough so that the variations will be much larger than the ionization potentials. Symon has shown that as the thickness gets less ~~that~~ the ratio of the rms fluctuation to the mean loss becomes infinite. The implication is that if the theory is used past its lower limit it will not predict wide enough fluctuations. Such seems to be the case.

Three things might be questioned about the conditions assumed when that calculation was made; (1) whether the spectrum is as assumed, (2) if it is true that only mesons are important, and (3) whether or not equipmental errors might enter in.

That the meson spectrum might be different than that used is quite possible. If one considers Wilson's data and the curve which Rossi has drawn through it (19,20), one realizes other curves could have been drawn through the same points. In particular one might easily think that the data indicates fewer low momentum mesons and more higher momentum ones than Rossi indicates. Making such a change would widen the expected fluctuation curve.*

That electrons are actually present is seen from inspection of the pictures concerned. Some are definitely identifiable for they show a measureable momentum that does not change appreciably in passing through the .89 gm/cm^2 of the counter. The number and relative distribution of these will be uncertain, however. Those present will probably have been produced locally, there being 320 gm/cm^2 of concrete above. The effect of these on the pulse height distribution observed might well be in either direction.

---

* This follows from the details of the calculations. See the last paragraph of Appendix B.

Certain troubles in the equipment might affect the experimentally observed curve of fluctuations. The amplifier might vary somewhat in amplification due to tube aging or the voltage to the proportional counter might drift slightly. There might be random effects. Since these readings were spread out over a time span of six months such influences are quite probable. This sort of effect would spread out the curve as measured.

Of these four effects mentioned, if they could be allowed for, one would have little effect on the agreement of the calculated and the observed curves, one is indeterminate and two would make it better.

Fortunately there is another piece of theory which gives an estimate of the ideal case in which the equipment is working perfectly and stably. In all theories of energy loss, the loss is divided into two kinds, high energy losses due to close interactions and low energy losses due to distant ones.* Close collisions happen seldom but are potent; they result in little knots of ionization or δ-rays scattered at finite intervals along the track. Distant collisions happen frequently; they result in an energy loss spread out fairly continuously along the track. It is further shown that roughly equal amounts of energy are lost by each process. Thus for path lengths short compared to the average interval in which happen large energy losses, only the one type will usually be observed. Thus the mean loss will be roughly twice the most probable energy loss for short path lengths.

---

* These comments are based on two seminars given by R.F. Christy of the Institute.

The present case is a short path length in the above sense. Let us then examine the ratio of mean to probable energy loss. A calculation made on the predicted curve shows this ratio to be 1.4, and one made on the observed curve gives it as 2.9. Presumably the ideal is somewhere in between.

4.5 Other experiments.

In the literature is very little experimental work which parallels this work. Much exists on range straggling and on the inhomogeneity introduced into homogenous beams by foils of metal, but these do not apply. However in the published results of two Russians is work that is quite close. N. Dobrotin (22) has described experiments with proportional counters detecting cosmic rays in which a curve of fluctuations is obtained. His differentiation of particles is as to whether they are of the hard component (8 cm of lead) or not. To this he fitted a curve calculated from Landau's theory, finding it too narrow and its tail too low. One cannot tell how much it was so, for there is neither graph nor data given of the comparison. He does give a small figure of the fluctuations themselves, which is given in its original size in fig. 11.

S. I. Nikitin (23), in an attempt to verify the varitron hypothesis, publishes some fluctuation data. He too compares his data to Landau's theory, and prints several figures showing the comparison. One such, for particles in the hard component (5.4 cm of lead), is given in fig. 12, in its original size. It is difficult to tell how great are his variations, for these figures are small and the comparison is carried out only to twice the maximum. What is seen there appears to have variations about as great as those obtained in this work.

Each of these men used gas thicknesses comparable to ours, though Nikitin's was spread out over 15 cm of path length. The two had other interests in doing this than cloud chamber control.

4.6 Conclusions

Fluctuations in ionization are great, greater than would be expected from the extrapolation of existing approximate theoretical calculations. As a result the measurement of the ionization produced by a particle along a small part of its path length is not a good indication of its mean ionization or of its most probable ionization. Data so obtained cannot be used without severe systematic error in determining the masses or velocities of single particles. Nevertheless if the sensitivity of the counter is adjusted to select particles of say four times minimum and above, the counter will select low energy events satisfactorily. Because the trailing edge of the fluctuations curve is long, one will still get some pictures of minimum ionization (in section 3.2's case about 2% of all these, or about 70% of the resultant pictures). At the same time since the leading edge is sharp practically none of the rare events with high ionization will be lost.

REFERENCES

1. W. Gentner, H. Maier-Leibnitz, and W. Bothe, Atlas Typischer Nebelkammerbilder, Berlin, Julius Springer, 1940.

2. C.R. Skobelzyn, Z. f. Ph. 54, 686 (1929).

3. P.M.S. Blackett and G.P.S. Occhialini, Nature 130, 363 (1932).

4. C.D. Anderson, Phys. Rev. 41, 405 (1932); 44, 5 (1933).

5. R.V. Adams, C.D. Anderson, P.E. Lloyd, R.R. Rau, and R.C. Saxena, Rev. Mod. Phys. 20, 334 (1948).

6. R.V. Adams, Thesis, CIT 1948.
   R.R. Rau, Thesis, CIT 1948.

7. A.T. Biehl, R.A. Montgomery, H.V. Neher, W.H. Pickering, and W.C. Roesch, Rev. Mod. Phys. 20, 353 (1948).

8. L.D. Statham, Rev. Sci. Inst. 19, 116 (1948).

9. S.A. Korff, Electron and Nuclear Counters, New York, van Nostrand, 1946.

10. C.D. Anderson, R.V. Adams, P.E. Lloyd, and R.R. Rau, Phys. Rev. 72, 724 (1947).

11. N. Bohr, Phil. Mag. 25, 10 (1913).

12. E.J. Williams, Proc. Roy. Soc. (London) 125, 420 (1929).

13. E.J. Williams, Proc. Roy. Soc. (London) 130, 310 (1931); 130, 328 (1931).

14. J.A. Gaunt, Proc. Camb. Phil. Soc. 23, 732 (1927).

15. H. Bethe, Ann. d. Ph. 5, 325 (1930).

16. C. Møller, Ann. d. Ph. 14, 531 (1932).

17. L. Landau, J. Phys. U.S.S.R. 8, 201 (1944).

18. K.R. Symon, Thesis, Harvard University 1948.

19. J.G. Wilson, Nature 158, 415 (1946).

20. B. Rossi, Rev. Mod. Phys. 20, 537 (1948).

21. E.J. Williams, Phys. Rev. 58, 292 (1940).

22. N. Dobrotin, J. Phys. U.S.S.R. 10, 207 (1946).

23. S.I. Nikitin, Zhurnal Eksperimental'noi i Teoreticheskoi Fiziki 18, 577 (1948).

APPENDIX A.

Estimation of the differential momentum spectrum for mesons at the equipment.

Several momentum spectra for mesons are given in the literature (see Rossi, ref. 20, p. 542 et seq.), but these are given either at some altitude or at sea level with the air only overhead. Our equipment was located on the first floor of East Bridge, a three story building. The question is, then, how all this matter above the chamber will affect the momentum distribution of the particles it sees.

The first question is just how much material is actually there. To this end, the structural drawings of the building were examined and checked with actual measurements on the spot, the latter being necessary because the drawings are not in every particular correct. From this information two scale drawings were made of cross-sections through the building passing through the chamber. These drawings made it possible to determine how much concrete lay between the chamber and the sky in any given direction.

Knowledge of the geometry of the counter arrangement permitted a determination of the angles θ_1 (limiting angle at which the upper counter entirely subtends the lower) and θ_2 (the angle at which neither counter subtends any part of the other). These angles in the long and the narrow dimensions were:

$$\theta_1 = 20.3^\circ \qquad \theta_1' = 3.0^\circ$$

$$\theta_2 = 37.6^\circ \qquad \theta_2' = 8.5^\circ$$

Then the relative probability of finding a particle in any direction θ measured in the wide direction of the counters is:

$$P(\theta) = \frac{J(\theta)}{J(0)} \cos\theta$$

$$P(\theta) = \frac{J(\theta)}{J(0)} \cos\theta \left(\frac{a + b - h\tan\theta}{2b}\right)$$

$$P(\theta) = 0$$

In these expressions $J(\theta)/J(0)$ allows for decrease in intensity with increase of zenith angle θ ; this expression was taken to be $\cos^2\theta$. The $\cos\theta$ allows for the foreshortening of the amount of area through which the radiation might pass. The additional term allows for the fact that particles passing through the upper counter in directions $\theta > \theta_1$ can pass through only a portion of the lower counter. Here a and b are the half lengths of the upper and the lower counter respectively, and h is the distance between them.

From the scale drawings of the buildings it was determined how much material lay in every direction of interest. This was tabulated as $t(\theta)$. A numerical integration was then carried out:

$$t_{ave} = \frac{\int t(\theta)\, P(\theta)\, d\theta}{\int P(\theta)\, d\theta}$$

which results in an approximate result for the amount of concrete overhead. This resulted in a figure of 52 inches of reinforced concrete, which at a density of 150 pounds per cubic foot gives a thickness of 320 grams per square centimeter.

Now concrete consists of things like lime ($CaCO_3$), sand (SiO_2) and water, with about 4% by weight of iron. Absorption in matter depends on the ratio $\Sigma Z / \Sigma A$. Figuring on a 6 to 1 mix in the concrete, we get this ratio = 0.48. This figure is very close to that for aluminum. The point of this is that it is possible to figure the concrete as approximately equivalent to so much aluminum.

The presence of an absorber will change the distribution of momenta observed under it by slowing down individual particles and possibly too by production of new particles in it. The former change is what is figured here, as it is something about which there exists definitely formulated theory.

The problem is: To each old momentum p' corresponds a new momentum p which is a definite function of p' and of the absorbing thickness t.

A distribution $n(p')\,dp'$ is known of the probability of finding a particle in the momentum range from p' to $p'+dp'$. To this is to be related a corresponding new probability distribution $n(p)\,dp$. If p and dp are the new momentum and momentum interval corresponding to the old ones, p' and dp', then

$$n(p)\,dp = n(p')\,dp'$$

or

$$n(p) = n(p')\frac{dp'}{dp}$$

To perform these operations, then, one needs a table or graph giving p' as a function of p, and another giving dp'/dp as a function of p'. Thus if $n(p')$ is plotted on doubly logarithmic paper, the operation is very quick. One carried the

the ordinate corresponding to the abscissa p' over to p , then goes up or down on the same new abscissa by a distance equal to the scale factor dp'/dp .

The result of these operations is given in Fig. 7.

APPENDIX B.

Fluctuation curve predicted.

As indicated on page 22 the prediction of the probability $N(\epsilon)\,d\epsilon$ of a loss between ϵ and $\epsilon + d\epsilon$ reduces to the integral

$$N(\epsilon) = \int P(p,\epsilon)\, n(p)\, dp$$

Here $n(p)$ is the result obtained in Appendix A, and $P(p,\epsilon)$ is contributed from the theory of Landau and Symon.

Symon gave a graph and a table of the function $\frac{\sigma_w}{F} P(\epsilon)$ versus $\frac{\epsilon - \epsilon_p}{\sigma_w}$ (all notation his), where

$$\sigma_w = b\xi \qquad \xi = \frac{Ne^4}{mv^2}\frac{Z}{A}\rho t$$

$$\epsilon_p = \xi\left(\ln\frac{\xi}{\epsilon} + j\right) \qquad = \text{most probable energy loss.}$$

$$\epsilon = \frac{I^2 e^{\beta^2}}{2mc^2(w^2-1)} \qquad w = \frac{1}{\sqrt{1-\beta^2}}$$

I = the average ionization energy of the absorber

j = 0.373 for thin foils

b = 1.48 for thin foils

F = 0.663 for thin foils

For this case, the thickness of gas ρt = 5.59 mg/cm^2; Z/A = 0.45; I = 190 e.v. We then get

$$\xi = \frac{386}{\beta^2} \qquad \sigma_w = \frac{572}{\beta^2}$$

Next is calculated F/σ_w, ϵ_p, and σ_w for 212 mass mesons of nineteen different momenta evenly spread on a logarithmic scale between 30 and 30,000 Mev/c. Then a series of 19 tables were prepared of the variation of the function $n(p)\,P(p,\varepsilon)$ with ε for the different values of p. Graphs were made for interpolation purposes. From these a set of graphs of $pn(p)P(p,\varepsilon)$ were made, this time plotted on semi-logarithmic paper with ε fixed and p variable. In this form the evaluation of

$$N(\varepsilon) = \int_{-\infty}^{\infty} p\,n(p)\,P(p,\varepsilon)\,d\ln p$$

is possible by considering the areas. This was done with a planimeter, and the results normalized to a maximum ordinate of unity (Results in Table V and Figure 8).

We can check now on the contribution to this curve due to particles that would be expected to have high mean ionizing power. In section 3.2 it was suggested that particles of normal mean ionizing power up to 3 x minimum might be included in the experimental curve. For mesons, this corresponds to a momentum of 55 Mev/c. A consideration of the graphs of $pn(p)P(\varepsilon,p)$ shows that the contribution to $N(\varepsilon)$ due to momenta less than this limit is very small, and due to high momenta is large. To illustrate this point a sample of this function is given in Figure 12.

TABLE V

PREDICTED ENERGY LOSS DISTRIBUTION

E	N(E)	E	N(E)
3000	.000123	9,000	.192
3250	.000576	9,500	.135
3500	.00311	10,000	.113
3750	.0208	11,000	.0776
4000	.0632	12,000	.0544
4250	.220	13,000	.0406
4500	.415	14,000	.0315
4750	.600	15,000	.0252
5000	.750	20,000	.0103
5250	.863	25,000	.00603
5500	.961	30,000	.00376
5750	.975	35,000	.00266
6000	1.000	40,000	.00192
6250	.938	45,000	.00146
6500	.903	50,000	.00113
6750	.861	60,000	.000755
7000	.765	70,000	.000538
7500	.589	80,000	.000405
8000	.387	90,000	.000315
8500	.261	100,000	.000250

Fig. 1a. Safety Circuits

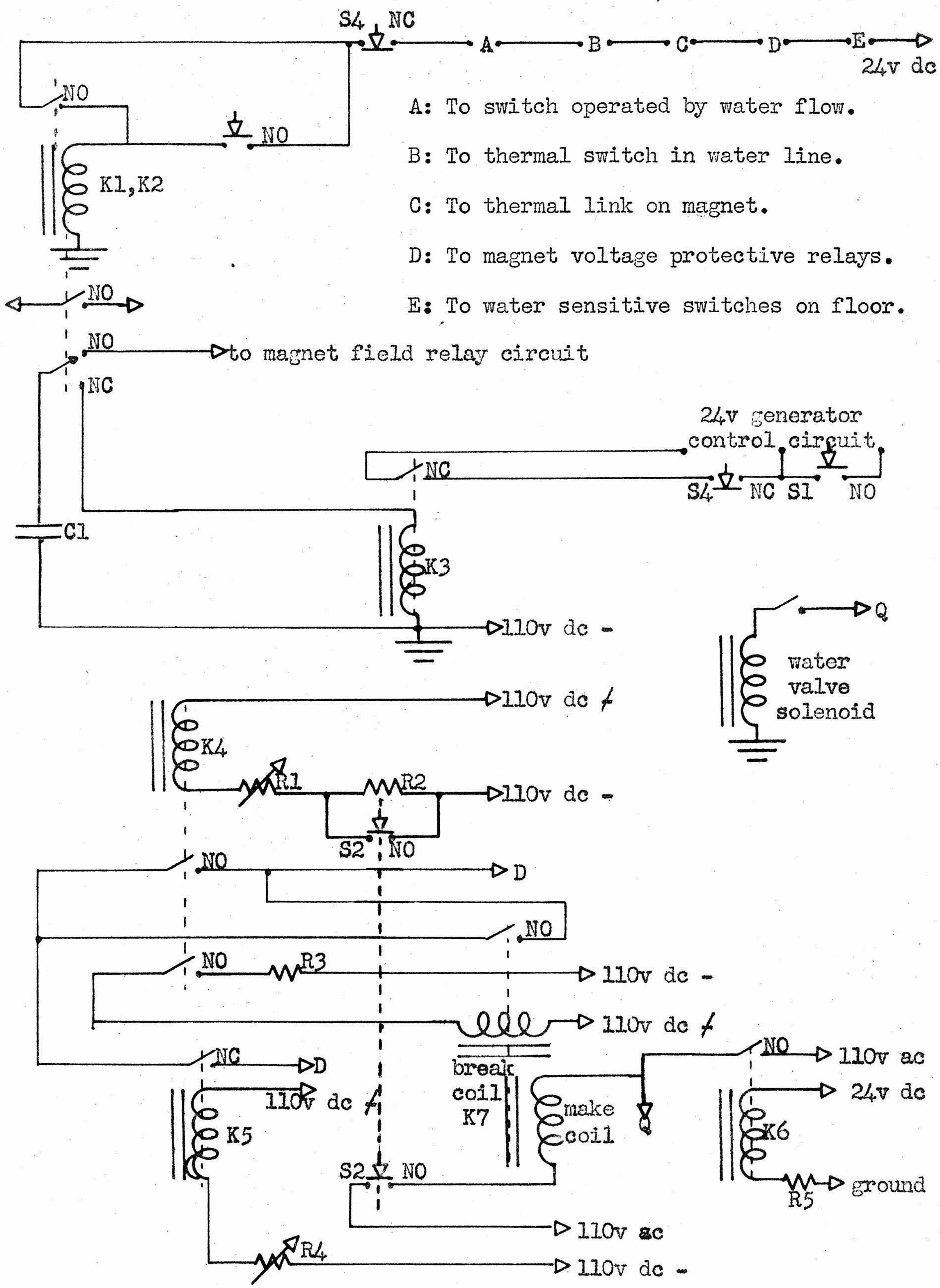

Fig. 1b. Safety Circuits

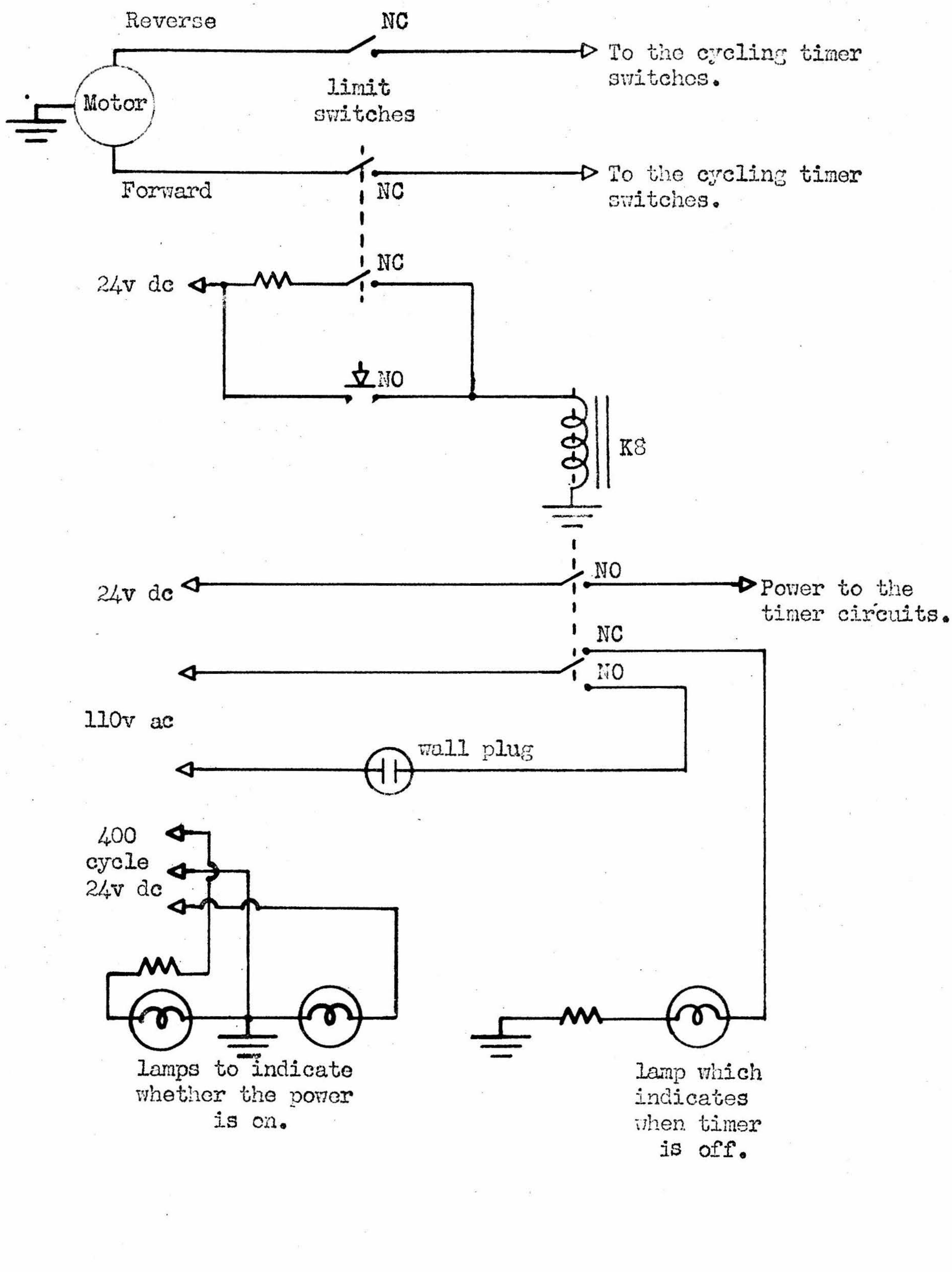

Fig. 2. The Proportional Counter

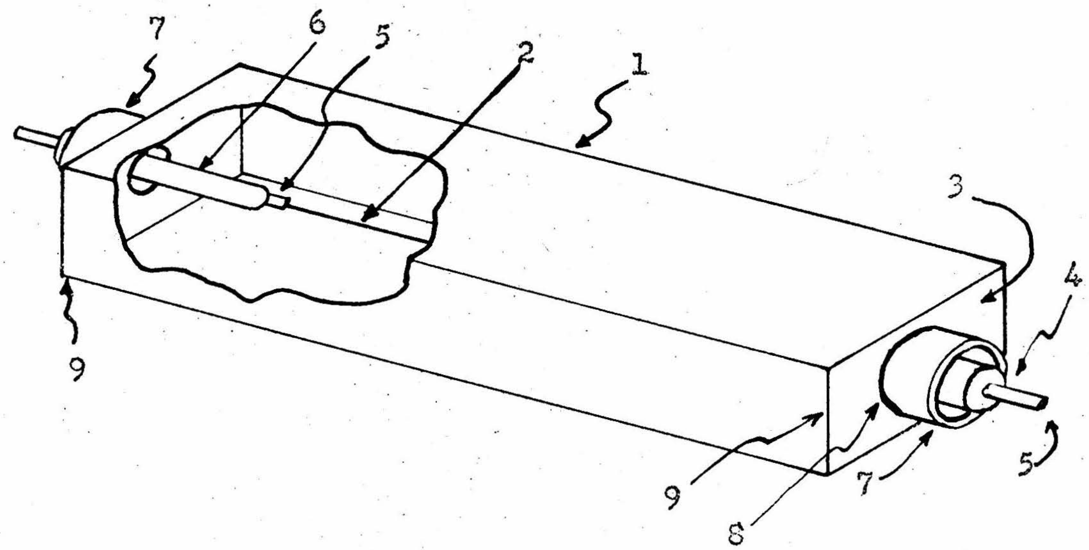

1. Metal cylinder formed from 1" o.d. 16 gauge SO aluminum tubing, squared and copper plated.
2. Tungsten wire 0.001 in. in diameter.
3. Flat copper ends.
4. Kovar eyelet containing glass bead.
5. Small Kovar tubing.
6. Glass covering to Kovar tubing.
7. Brass cylindrical ring for mounting.
8. Silver soldered joints.
9. Tin--lead soldered joints.
10. Filling tube, pinched off to a feather edge, and seal reinforced with solder. (Not shown on this drawing.)

Fig. 2b. The proportional counter.

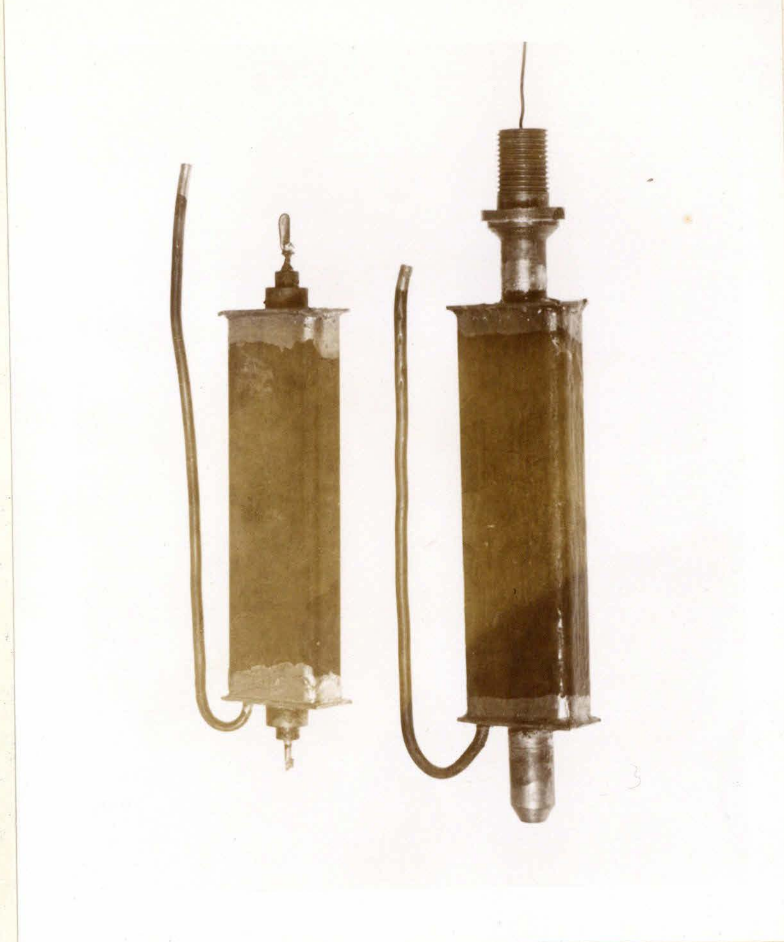

Two unfilled tubes are shown in successive stages of their manufacture. The one on the right has had brass sleeves mounted on each end. The lower one is protective, shielding that end from pickup and from dust and moisture. The upper one also serves to mount the tube on the glass of the chamber and to provide electrical connections.

Fig. 3a. Counter mounting, disassembled.

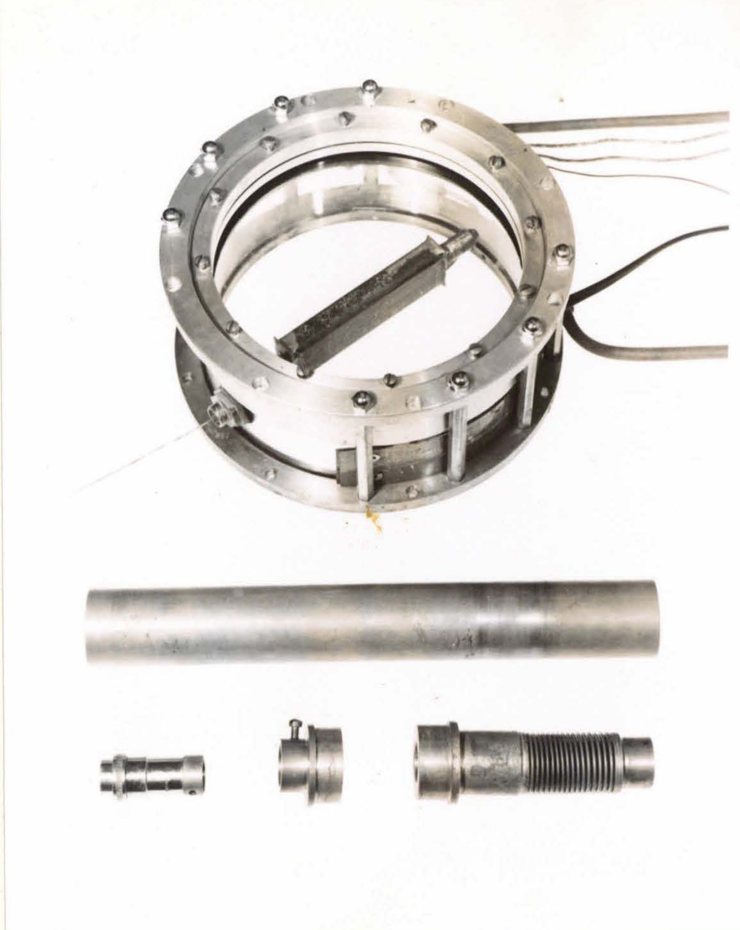

The counter is seen in place in the chamber. One can see washers whose faces are curved to fit the glass of the chamber. The components of the electrical connections and shielding are shown separately. These consist of a flexible coupling, a long sleeve, and connectors to lead the signals into the preamplifier.

Fig. 3b. Counter mounting, assembled.

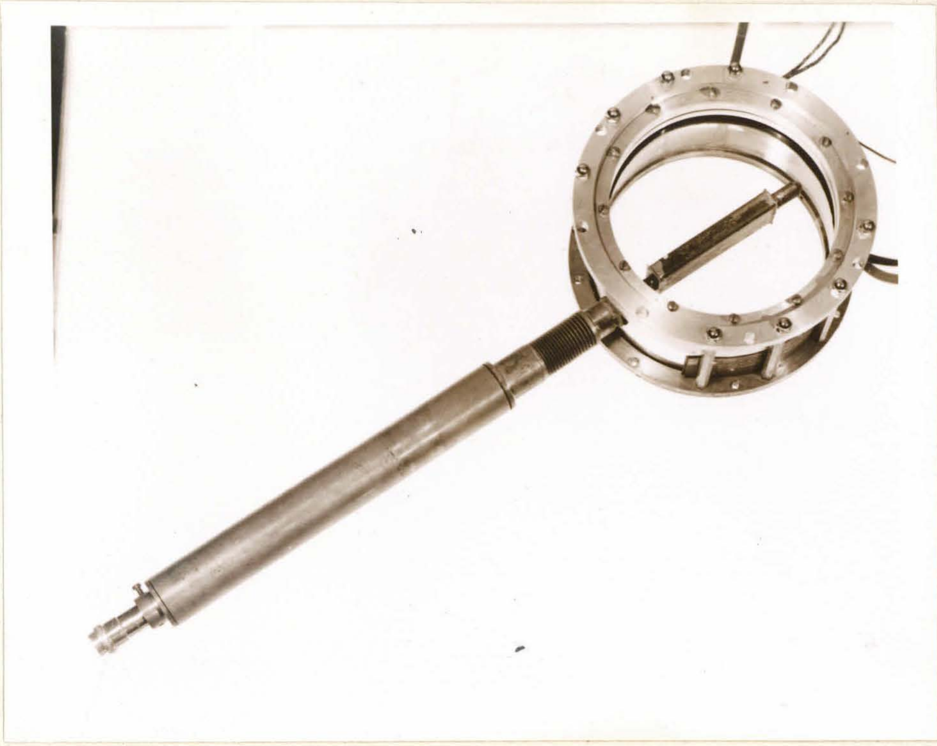

The counter is shown in the chamber. Connected to it are the lead-out wire and its shielding.

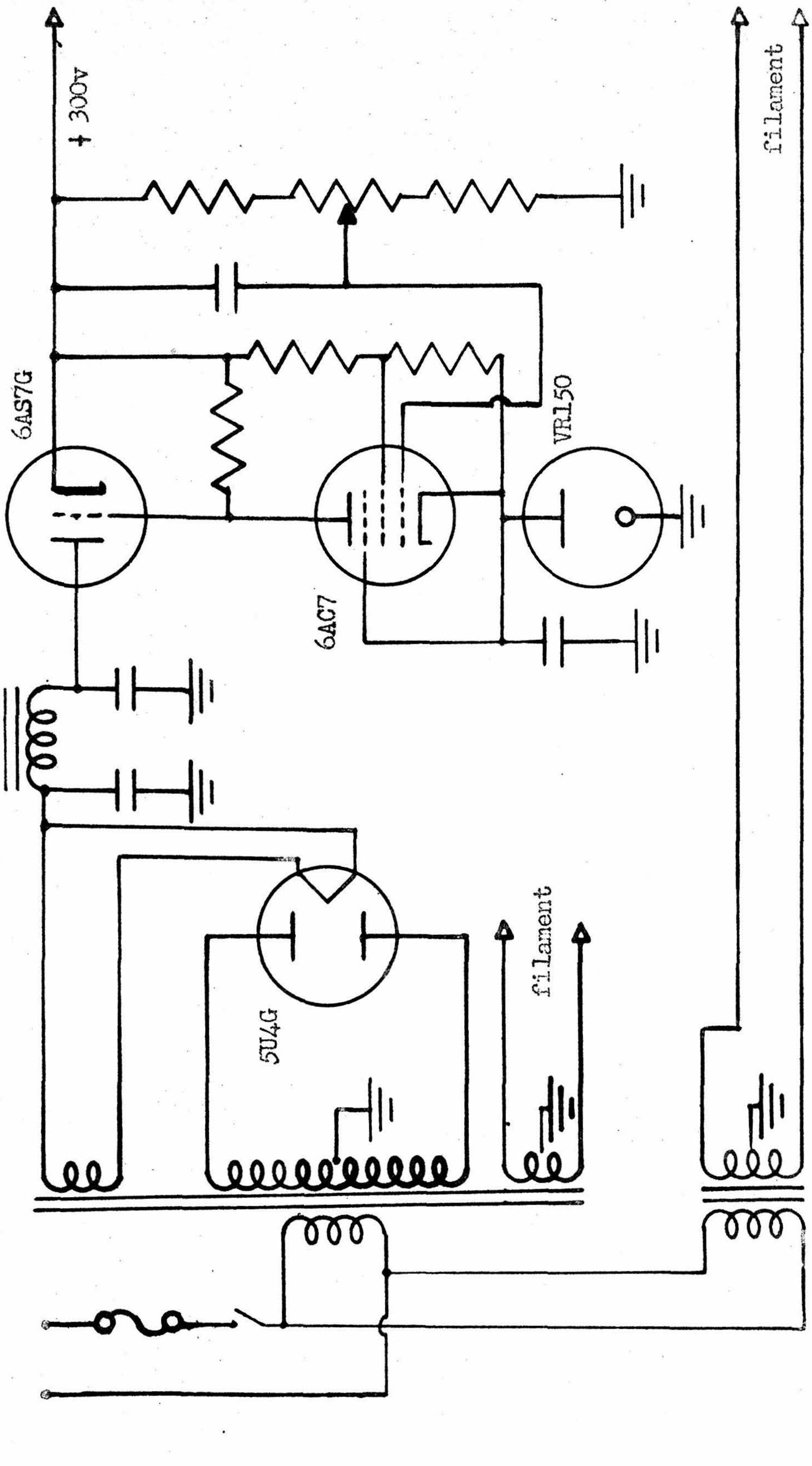

Fig. 4a. Amplifier Power Supply

Fig. 4b. Preamplifier Power Supply

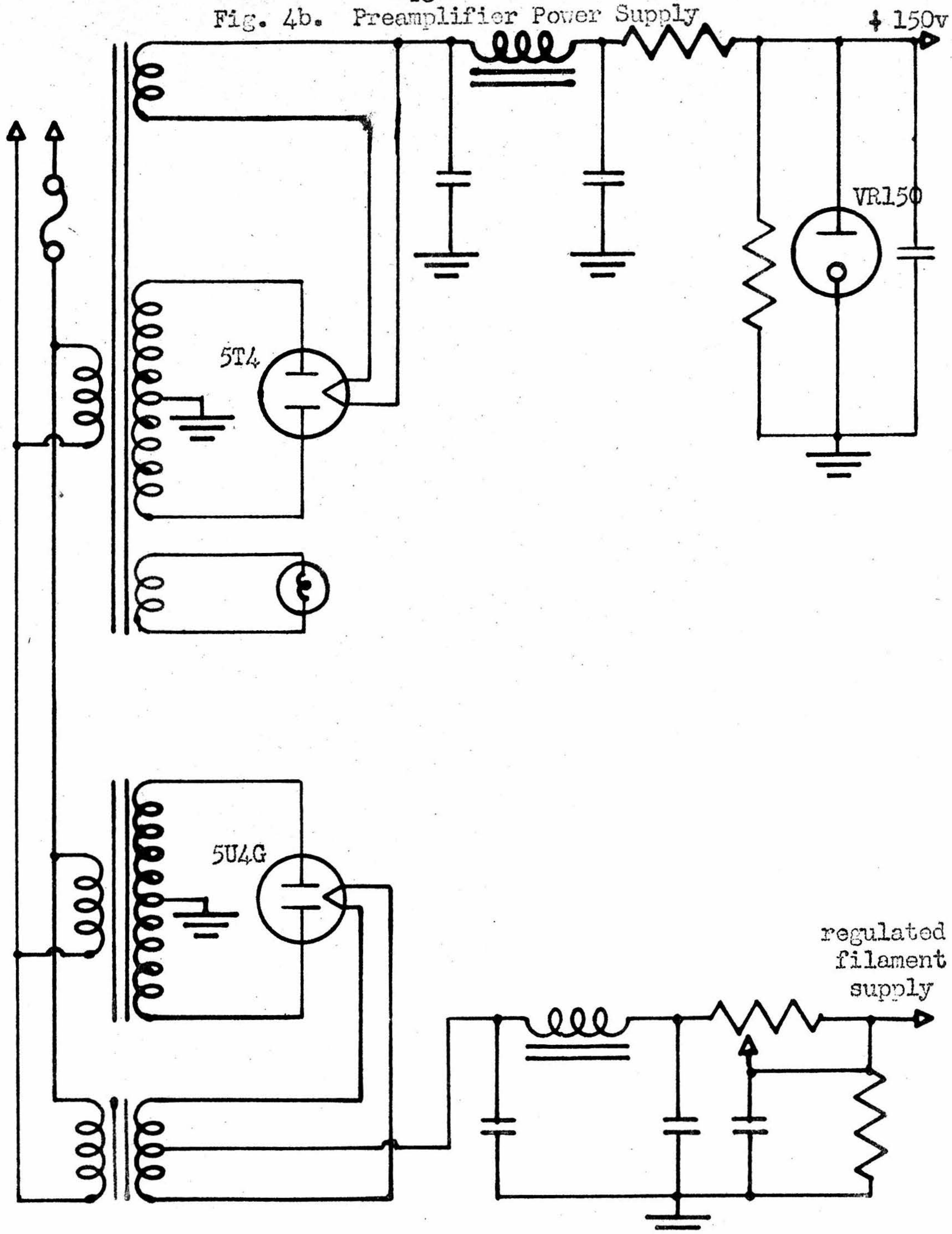

Fig. 4c. Preamplifier

All tubes 6AK5.

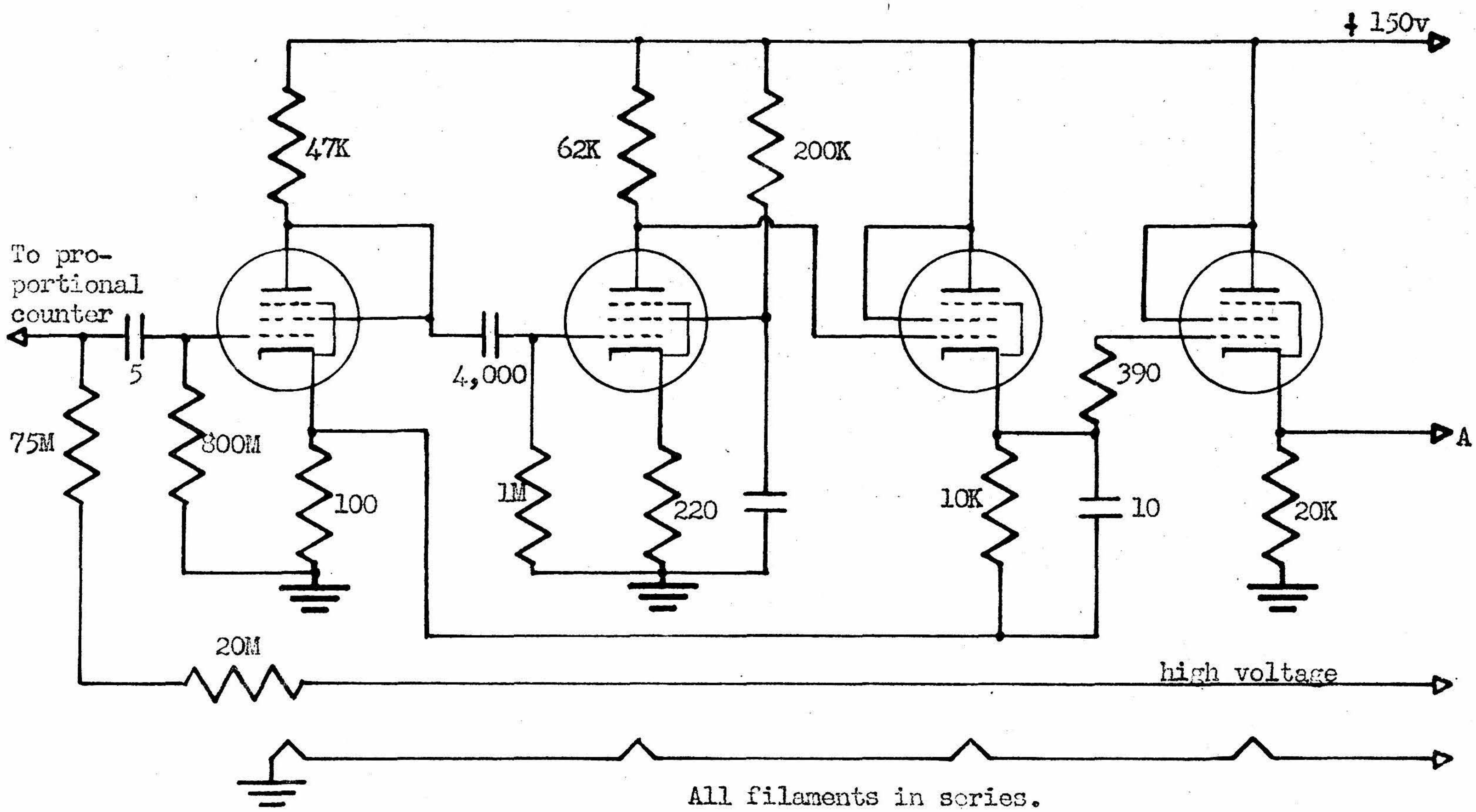

All filaments in series.

Resistor values in ohms.
Condenser values in micro-microfarads.
K = x 1000 ; M = x 1,000,000

Fig. 4d. Amplifier

All tubes, except 1, 6AC7

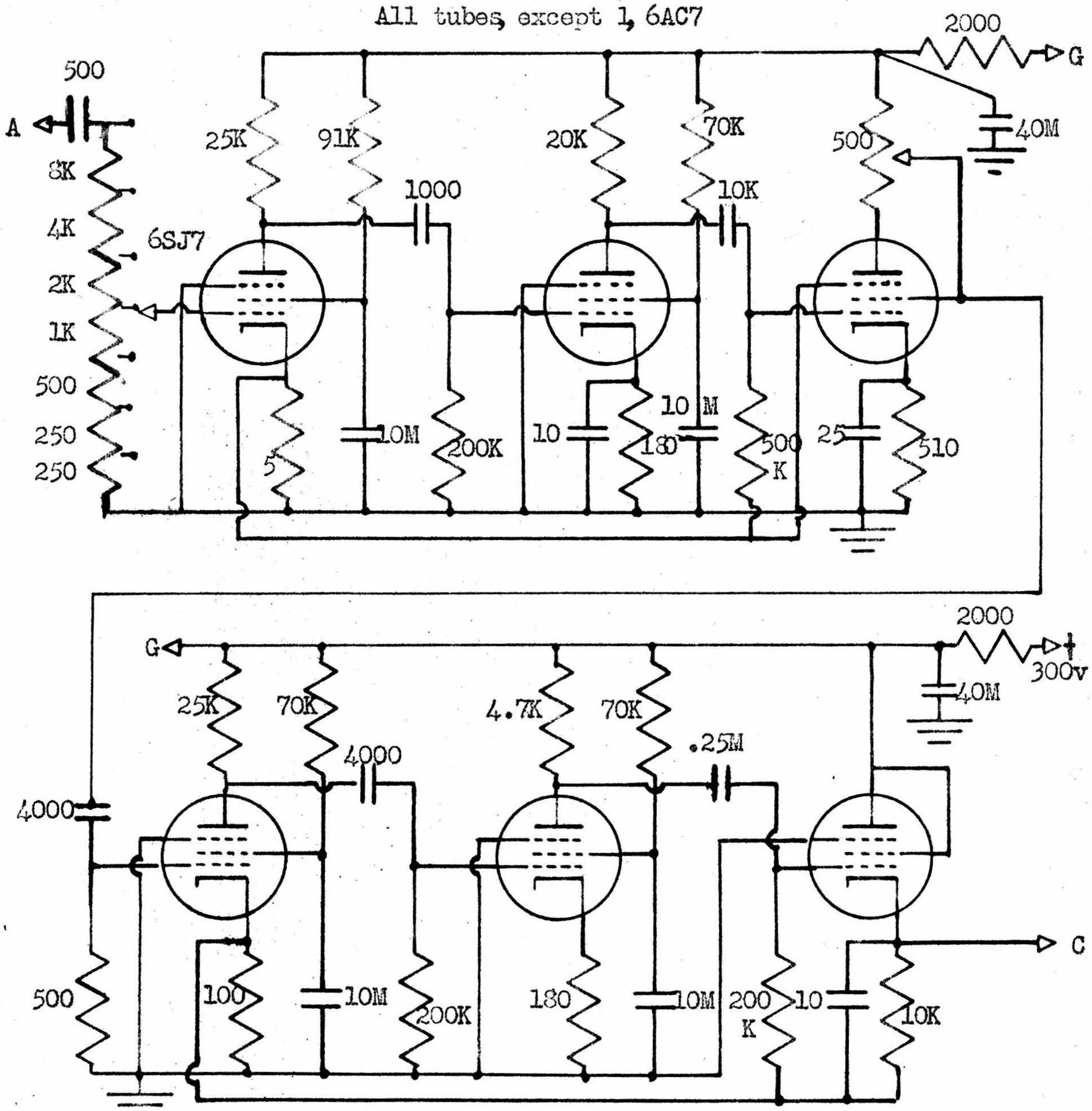

Resistor values in ohms.
Condenser values in micro-microfarads.
K = x 1000 ; M = x 1,000,000

Fig. 4e. Coincidence and Gate Circuits

All tubes ½ of 6SN7

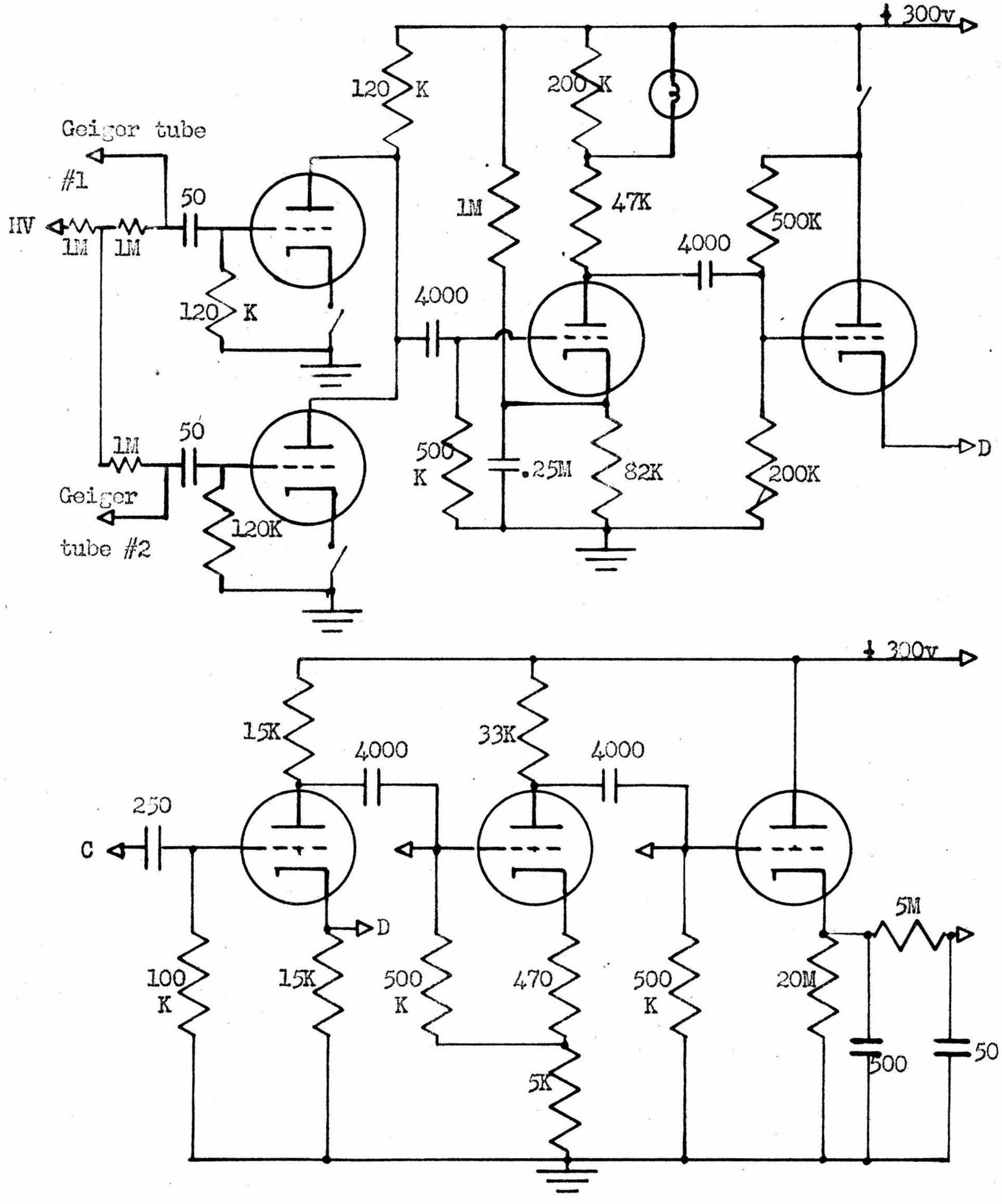

Resistor values in ohms.
Condenser values in micro-microfarads.
K = x 1000 ; M = x 1,000,000

Fig. 4f. Metering and trip circuits.
All tubes 1/2 of 6SN7 or 6H6.

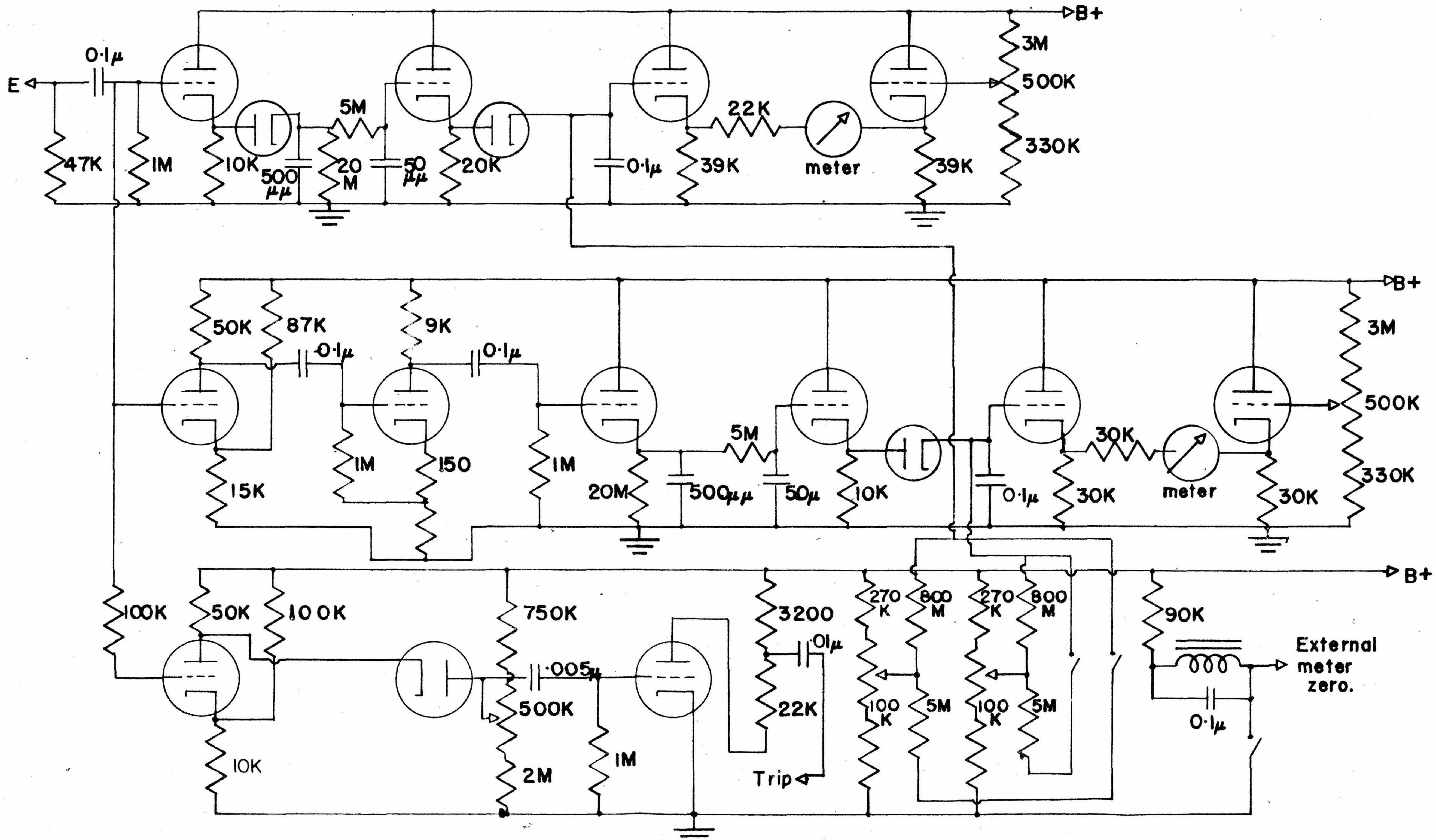

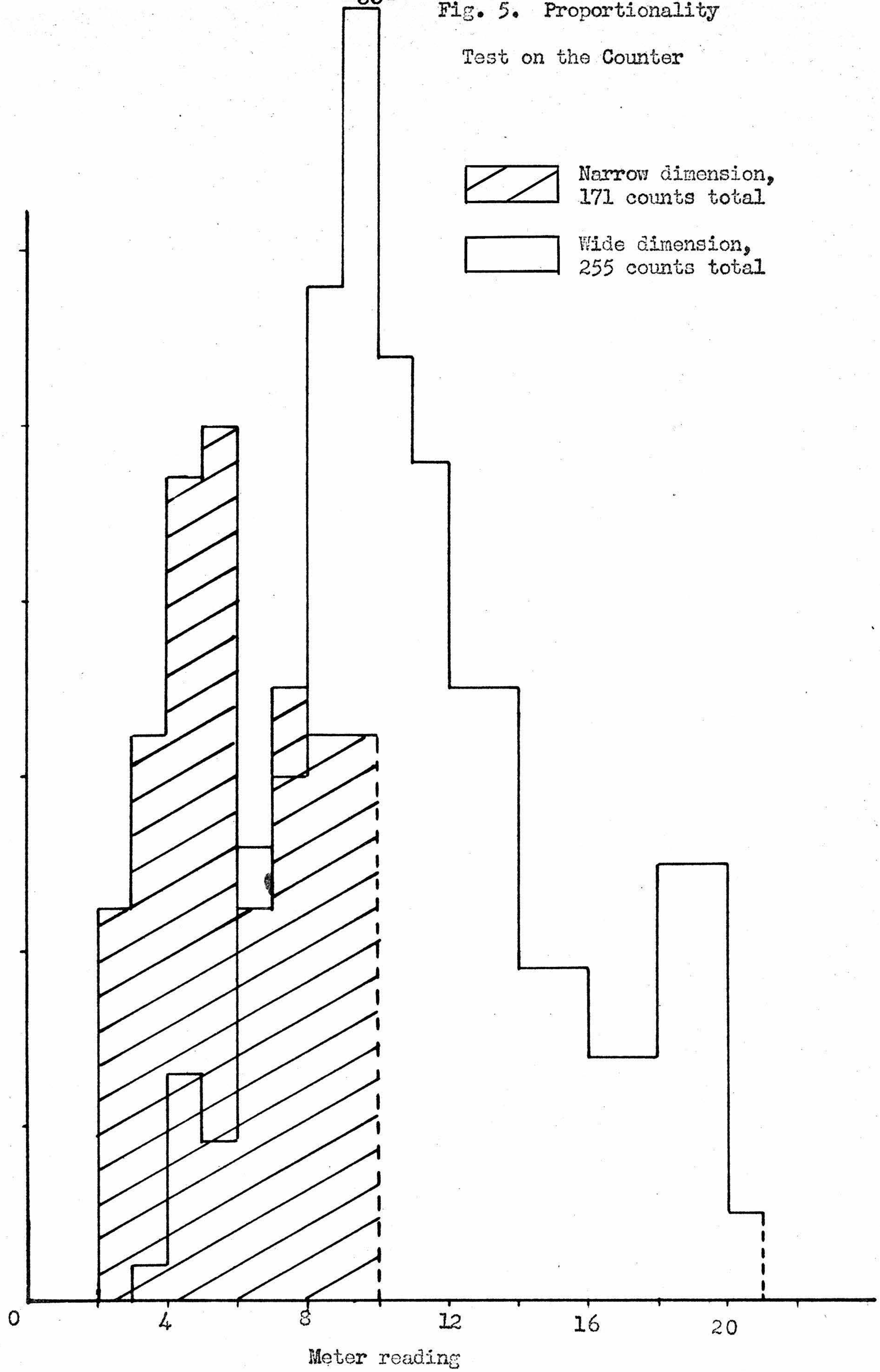

Fig. 5. Proportionality Test on the Counter

Fig. 6. Proportional Counter Test

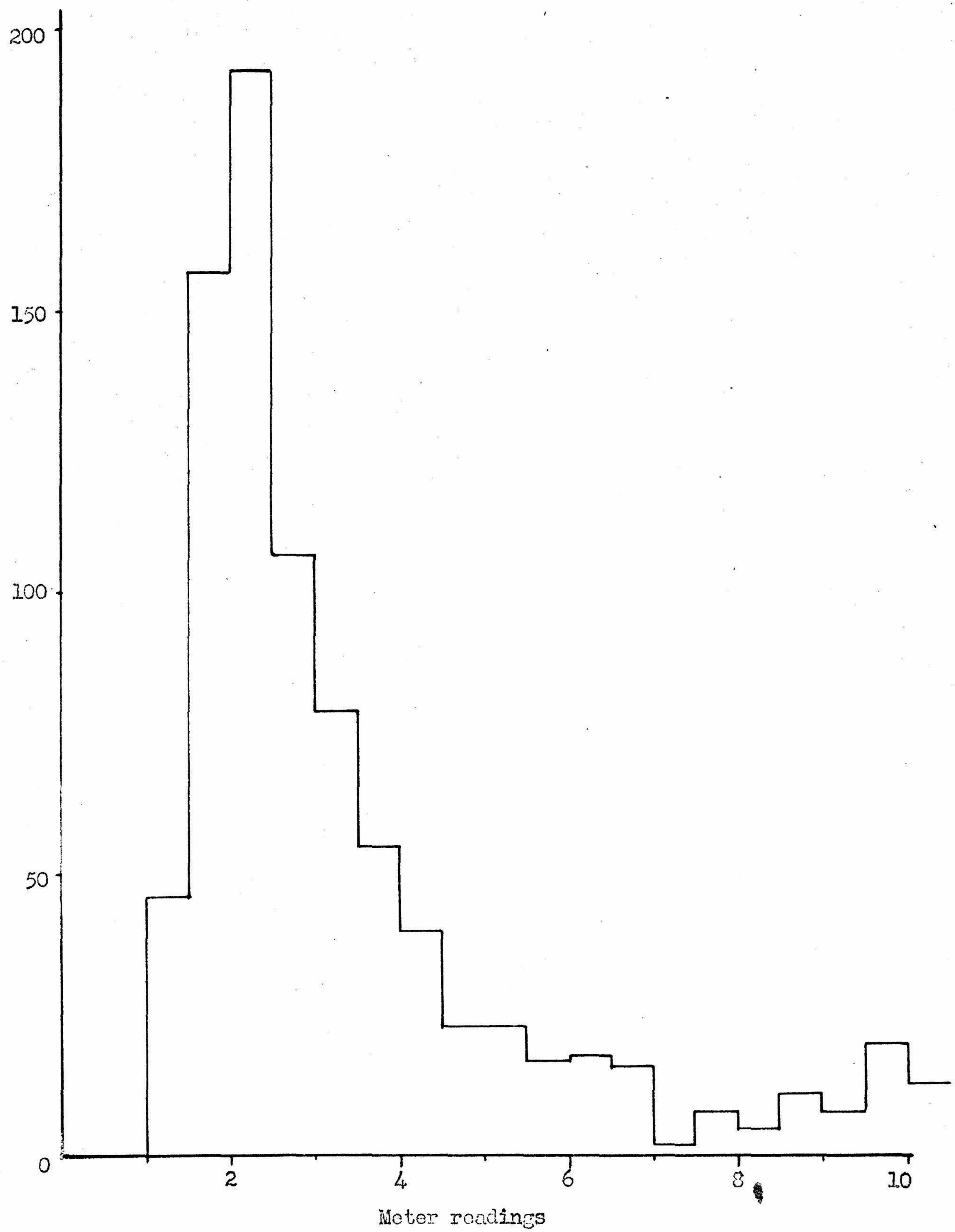

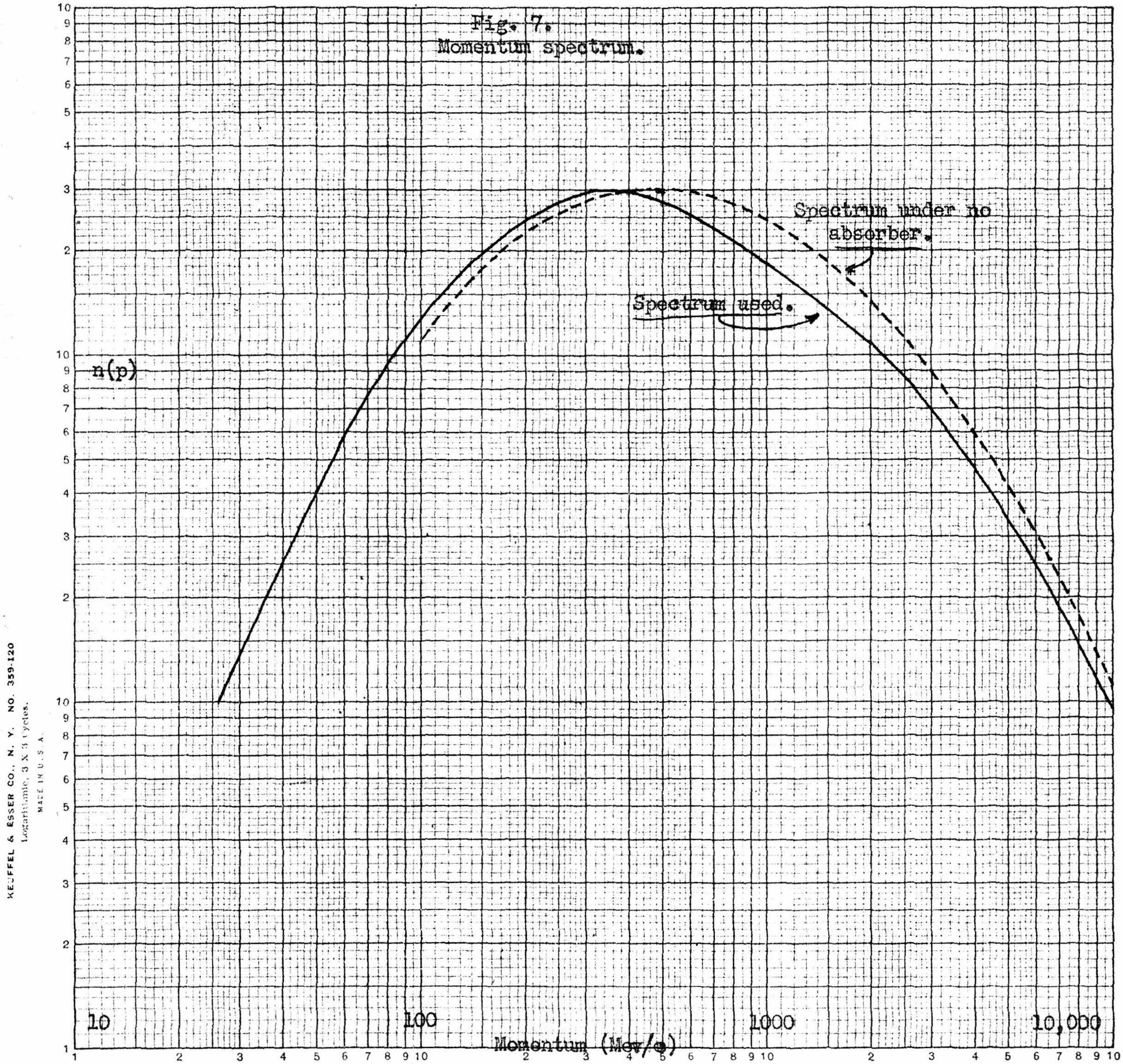
Fig. 7.
Momentum spectrum.
Spectrum under no absorber.
Spectrum used.
n(p)
10
100
1000
10,000
Momentum (Mev/c)
KEUFFEL & ESSER CO., N. Y. NO. 359-120
Logarithmic, 3 X 3 Cycles.
MADE IN U. S. A.

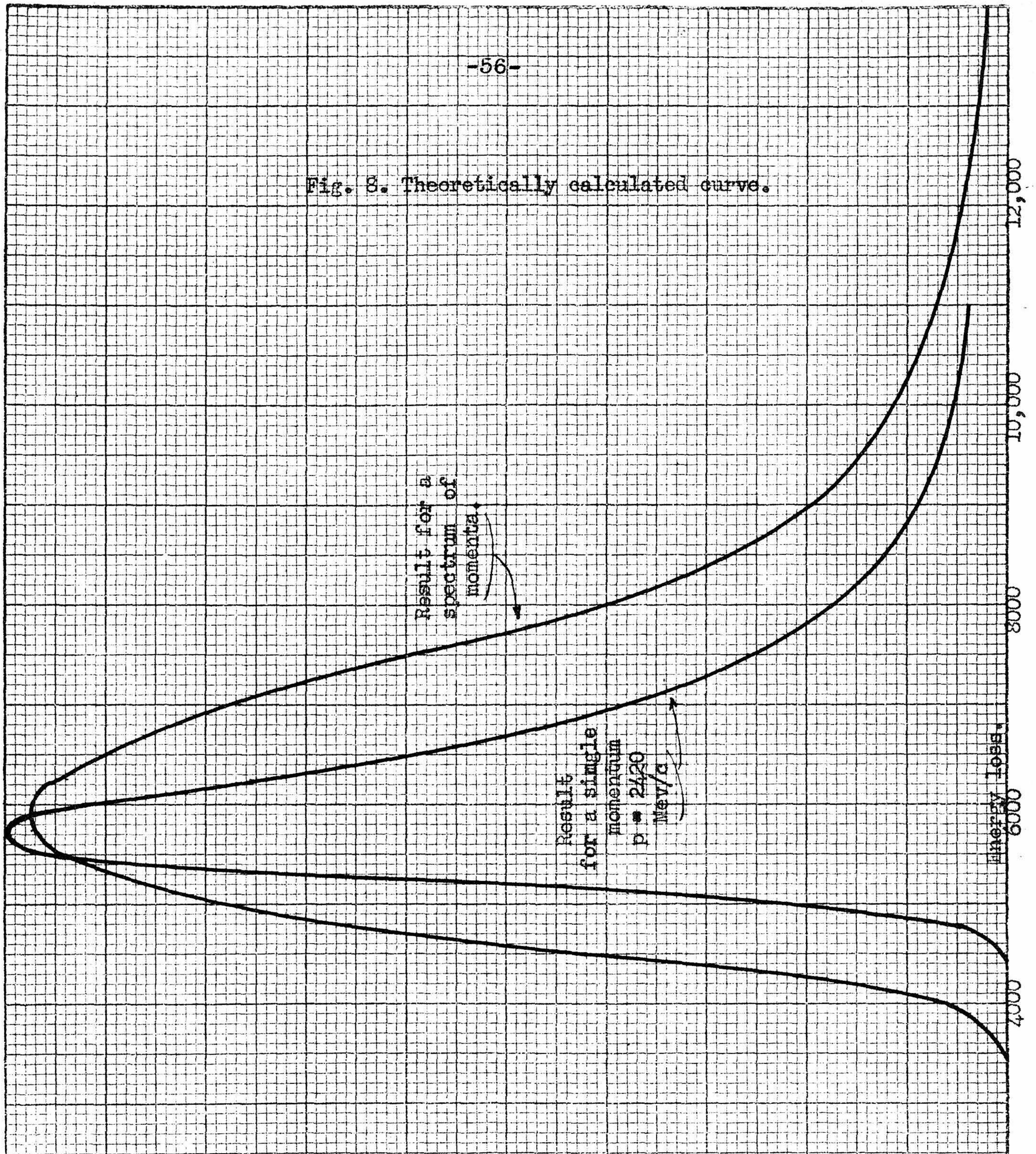

Fig. 8. Theoretically calculated curve.

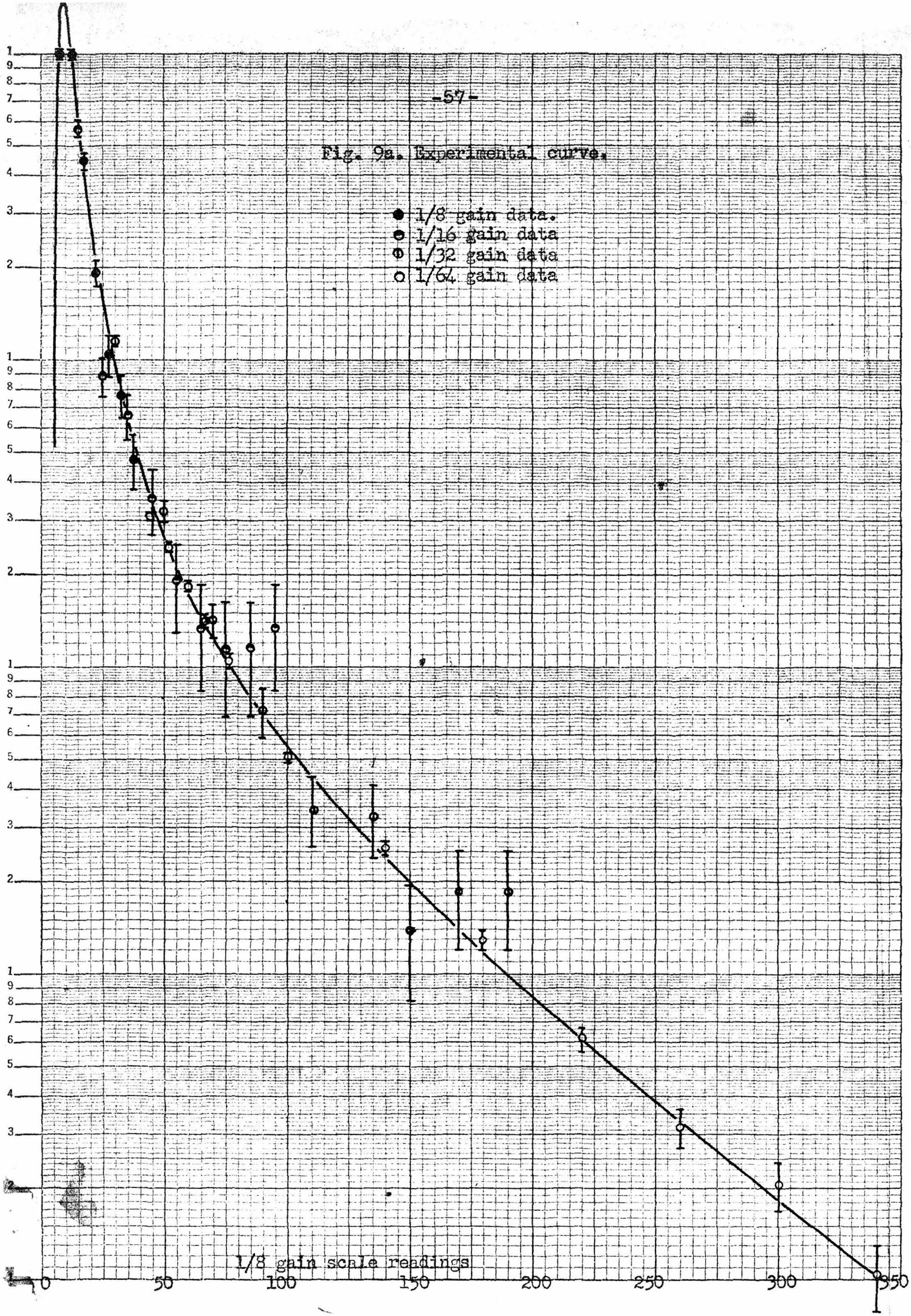

Fig. 9a. Experimental curve.

Fig. 9b. Experimental curve.

Only the 1/8 gain and the 1/64 gain data are plotted.

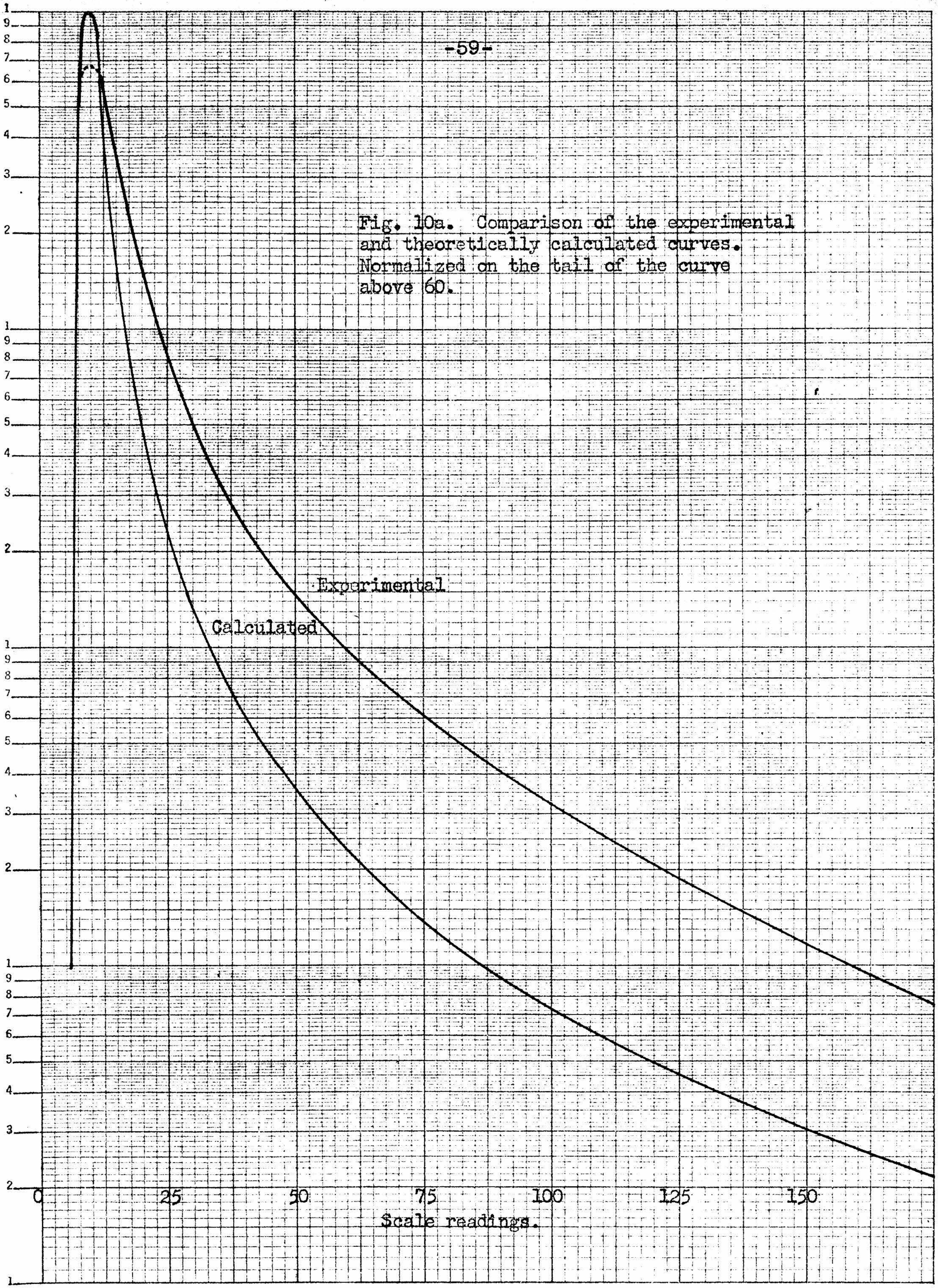

Fig. 10a. Comparison of the experimental and theoretically calculated curves. Normalized on the tail of the curve above 60.

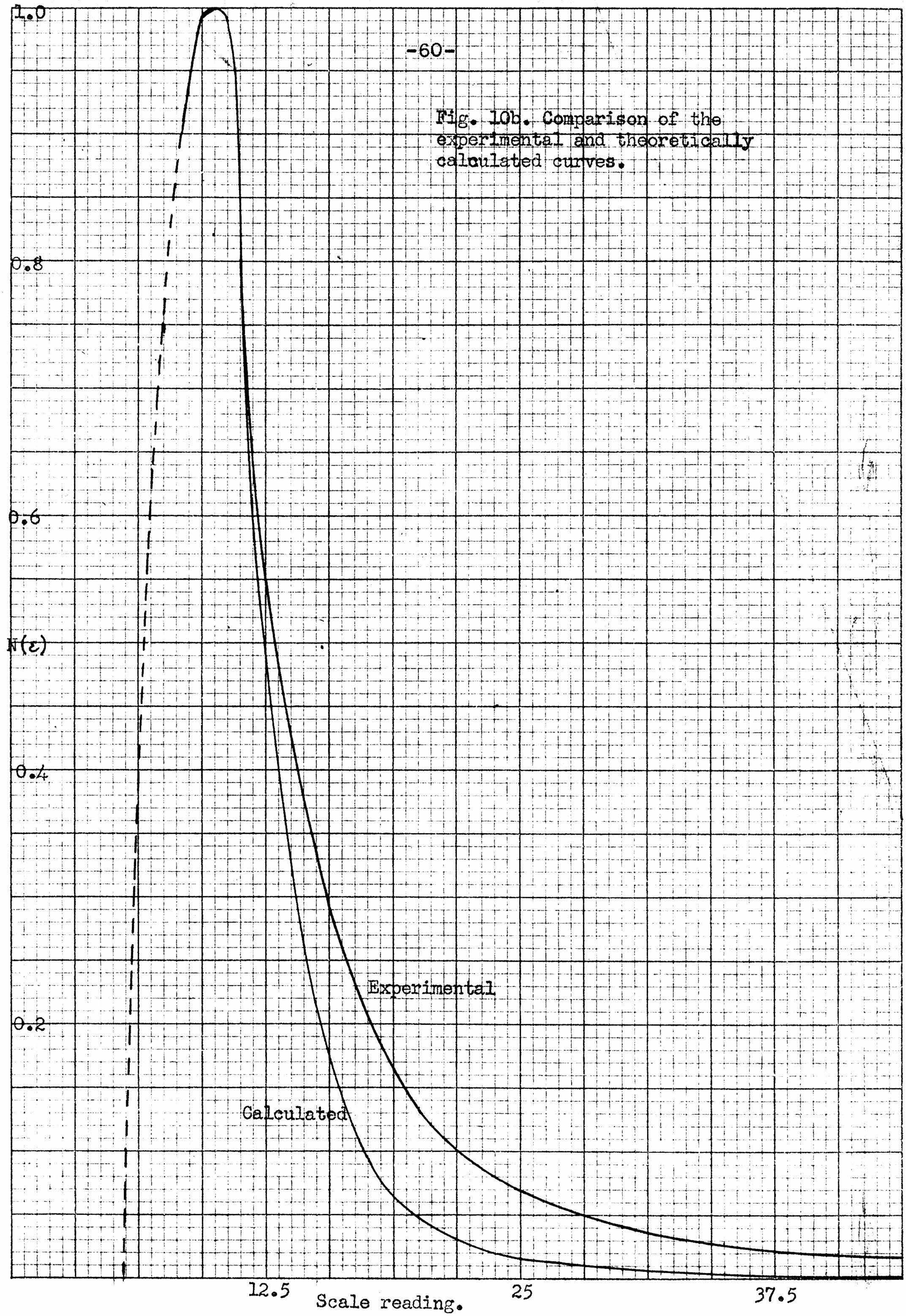

Fig. 10b. Comparison of the experimental and theoretically calculated curves.

Fig. 11. Data of Dobrotin and Nikitin.

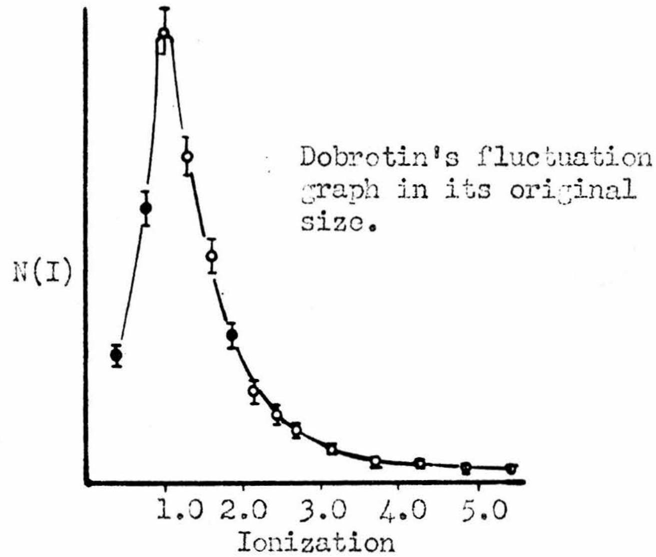

Nikitin's fluctuations.

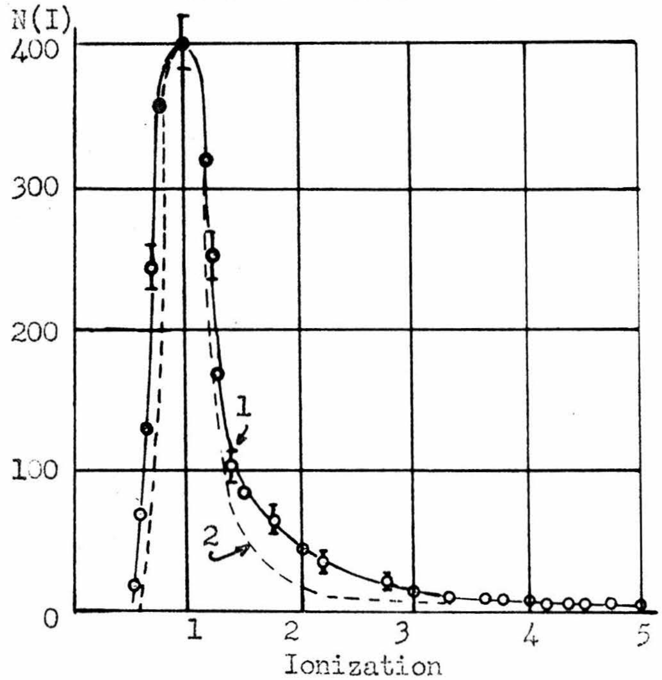

1: experimental curve.
2: theoretical curve.

Fig. 12. Sample curves

of the function pn(p)P(ε,p).